Mechanics and Mechanical Engineering
Vol. 7, No. 2 (2004) 23–60

Instability of Darcian Flow in an Alternating Magnetic Field

Yusry O. EL-DIB and Osama E. ABD EL-LATIF
Department of Mathematics-Faculty of Science, King Saud University
Al-Jouf, Saudi Arabia
e:mail: oeabdellatif@hotmail.com
yusryeldib52@hotmail.com

Received (5 March 2004)
Revised (31 March 2004)
Accepted (19 May 2004)

This paper treats the stability of an interface between two different fluids moving through two different porous media. There is an alternating magnetic field parallel to the interface and to the flow direction, and there is a concentrated sheet of electric current at the interface which produces jump in the magnetic field strength. The evolution of the amplitude of propagation surface waves is governed by a complex Mathieu equation which have damping terms. In the limiting case of non-streaming fluids a simplified damped Mathieu equation has been imposed. At a critical value of the stratified magnetic field, the ordinary Mathieu equation without the damping terms is derived. The contribution of viscosity to the existence of free electric surface currents on the fluid interface is discussed. It is found that at the critical stratified magnetic field, the surface currents density has disappeared from the interface whence the stratified viscosity has a unite value. The stability criteria are discussed theoretically and numerically in which stability diagrams are obtained. Regions of stability and instability are identified for the wavenumber versus the coefficient of free surface currents. It is found that the increase of the fluid velocity plays a destabilizing influence in the stability criteria. Porous permeability and viscosity ratio play a stabilizing or a destabilizing role in certain cases. It is found that the viscosity ratio plays a dual role in the stability behaviour at the resonance case. The field frequency plays a stabilizing influence in the case of weak viscosity analysis and at a special value of the magnetic field ratio. The destabilizing influence for the field frequency is observed for the case of the Rayleigh-Taylor model and at the resonance case.

Keywords: porous media, stratified magnetic field, Matieu equation.

1. Introduction

The instability of the plane interface separating two fluids when one is accelerated towards the other or when one is superposed over the other has been studied by several authors. Chandrasekhar [1] has given a detailed account of these investigations. The instability of the interface may arise when the two fluids are in relative motion. The instability of the plane interface between two superposed fluids with

a relative horizontal velocity is called Kelvin-Helmholtz instability. The Kelvin-Helmholtz instability has been studied extensively for continuum, inviscid flows. The model for the classical Kelvin-Helmholtz instability involves a horizontal interface between two fluids with different parallel, uniform, horizontal velocities. In Kelvin-Helmholtz model, the effect of streaming is destabilizing in the linear sense (Chandrasekhar [1]). This instability, which arises as a consequence of a relative drift velocity of two fluids along the surface of discontinuity, has great relevance to various physical phenomena such as commentary tails and the magnetospherical boundary. The Kelvin-Helmholtz instability due to shear flow in stratified fluids has attracted the attention of many researchers because of its determinant influence on the stability of planetary and stellar atmospheres and in practical applications. The study of the Kelvin-Helmholtz instability has a long history in hydrodynamics. It is well known that in two-dimensional inviscid, incompressible hydrodynamics, there are two invariants of fluid motion. The existence of these two invariants requires that, in two-dimensional inviscid incompressible hydrodynamics, the energy cascades to long wavelength or vortices with similarly signed vorticity must tend to group together [2]. Indeed, hydrodynamic experiments have shown at the late stage of the Kelvin-Helmholtz instability two vertical structures that combine to form a single, larger vertical structure. Such a nonlinear evolution of the Kelvin-Helmholtz instability has been reproduced by numerical experiments and theoretical investigations [3].

The linear formulation of the Kelvin-Helmholtz instability in the context of magnetic fluids was investigated by Rosensweig [4]. His analysis revealed that the velocity difference that can be supported by the fluids before the instability sets in is enhanced if the difference in the permeability of the fluids across the interface and the strength of the applied magnetic field are increased. These fluids differ from magnetohydrodynamic fluids since no electric surface current flows in these fluids. The propagation of plane waves in magnetohydrodynamic fluids in the presence of a tangential magnetic field has been investigated theoretically as well as experimentally by Zelazo and Melcher [5]. These authors have demonstrated that the magnetic field exerts a stabilizing influence on the stability of the fluid surface. In their experiment, a plane wave of specific wavelength, consistent with the boundary conditions, was imposed on the interface, and the subsequent frequency shift for various strengths of the magnetic field was measured. Both theoretical and experimental results show an upward shift of frequency of the imposed wavelength as a function of the magnetic field.

In the comparable case of parallel flow, Drazin [6], Nayfeh and Saric [7] and Weissman [8] have studied the nonlinear development of the Kelvin-Helmholtz instability. In the presence of the vertical or the horizontal electric fields, Melcher [9] discussed the linear Kelvin-Helmholtz instability for continuum incompressible fluids. In one of the most recent works on this subject, the effects of periodic body forces were discussed. The effect of a time-dependent acceleration in the presence of tangential magnetic field on the nonlinear stability of Kelvin-Helmholtz wave has been discussed by El-Dib [10]. Recently, El-Dib and Matoog [11] have studied the Kelvin-Helmholtz instability for Maxwellian fluid sheet. They discussed the linear instability for the influence with the periodic electric field. In nonlinear evolution of the Kelvin-Helmholtz instability El-Dib [12] has demonstrated for dielectric vis-

coelstic interface.

Many technological processes involve the parallel flow of fluids of different viscosity, and density through porous media. Such flows exist in packed bed reactors in the chemical industry, in petroleum production engineering, in boiling in porous media and in many other processes as well. The flow through porous media is of considerable interest for petroleum engineers and in geophysical fluid dynamicists.

Should the interface between the two fluids become unstable, a substantial increase in the resistance to the flow will result. This increase in resistance, in turn, may cause flooding in counter current packed chemical reactors and dryout in boiling porous media. In the same vein, in petroleum production engineering, such instabilities may lead to emulsion formation. Hence, knowledge of the conditions for the onset of instability will enable us to predict the limiting operating conditions of the above processes. The purpose of this paper is to establish the condition for the onset of linear instability.

In all the works cited above, the medium is assumed to be non-porous. There are two reasons to extend these studies to media containing porous layers: (i) the Kelvin-Helmholtz instability is among the most simple and (ii) is the most frequently met in practice among motions in the presence of a porous medium. For excellent reviews about porous media, see refs. [13-15].

In contrast, the Kelvin-Helmholtz instability for flow in porous media has attracted little attention in the scientific literature. The instability of the plane interface between two uniform superposed fluids streaming through a porous medium was investigated by Sharma and Spanos [16], and the Kelvin-Helmholtz instability for flow in porous media was investigated by Raghaven and Mardsen [17] for Darcy-type flow. They used linear stability analysis to obtain a characteristic equation for the growth rate of the disturbance and then solved this equation numerically. They concluded that Kelvin-Helmholtz instability is possible only if the heavier fluid is over laying the lighter one (a statically unstable situation). This is obviously incorrect on physical grounds (possibly when Darcy's term is dominant). A linear theory of Kelvin-Helmholtz instability for parallel flow in porous media was introduced by Bau [18] for Darcian and non-Darcian flows. In both cases, Bau found that velocities should exceed some critical value for instability to manifest itself. A series of studies for Kelvin-Helmholtz instability have been initiated by Gheorghitza [19], and Georgescu and Gheorghitza [20], where uniform motions of inviscid, incompressible fluids and heterogeneous porous media are considered in several simple cases. In the presence of the horizontal electric field El-Sayed [21] re-discussed the Bau problem [18]. Recently, Mohamed et al. [22] studied the nonlinear Kelvin-Helmoholtz instability in porous media in the presence of both vertical and horizontal electric fields. This investigation is based on weak viscous effects. El-Dib and Ghaly [23, 24] investigated linear and nonlinear interfacial stability for flow in porous media in the presence of an oblique magnetic field. For arbitrary viscosity and in the presence of the vertical magnetic field, El-Dib [25] investigates the nonlinear Rayleigh-Taylor instability through porous media. Recently, El-Dib [26] reinvestigates nonlinear Rayleigh-Taylor instability in the presence of magnetic field parallel to the interface and to the flow direction, and there is a concentrated sheet of electric current at the interface.

The phenomena of parametric resonance arise in many branches of physics and

engineering. The treatment of the parametric excitation system having many degrees of freedom and distinct natural frequencies is usually operated by using the multiple time scales as given by Nayfeh [27]. The behaviour of such system is described by an equation of the Hill or Mathieu types [11] and [27]-[33]. It is well known that the stability of such solutions may be described by means of the characteristic curves of Mathieu curves which admit regions of resonance instability. The phenomena of interfacial stability in multilayer flow of magnetic fluids are of interest in many processing applications. The present work deals with the influence of an alternating magnetic field on fluid flows in a porous medium that is assumed to be more suitable in oil industry. A generalization of the Kelvin-Helmholtz instability for fluid flows in a porous is the goal in this study. In addition, the influence of free surface currents has been demonstrated in this investigation. This influence, for the presence of the surface current density, has been demonstrated before by El-Dib [28] and by El-Dib and Moatimid [29], for rotating magnetic fluid column in a continuum media.

2. Problem Statement and Basic Equations

We shall study two-dimensional progressive waves at the conducting interface $y = 0$, which separates two incompressible moving Darcian fluids. The Cartesian coordinates (x, y) are taken into consideration. By two-dimensional we mean that the flow field depends on the horizontal direction of propagation, which will be x-axis. The surface deflection is in the vertical y-direction and expressed by $y = \xi(x, t)$. We are interested in the interfacial response of the two phase's system after a disturbance of the equilibrium configuration. The equilibrium configuration is considered to be two immiscible fluids which have constant properties and occupy the half-spaces of uniform, homogeneous and isotropic porous media above and below a horizontal plane. The fluids move with two different uniform, horizontal, parallel velocities. The fluids are subjected to periodic tangential magnetic field.

$$\underline{H}^{(j)}(t) = \left(H_0^{(j)} + H_{00}^{(j)} \cos \varpi\, t\right) \underline{e}_x, \tag{1}$$

H_0 refers to the constant part of the field, $H_{00}^{(j)} (= \sqrt{\varepsilon} H_0^{(j)}$, ε is a small dimensionless parameter) is the amplitude of the periodic field and ϖ refers to the field frequency. The unit vectors $\underline{e}_x$ and $\underline{e}_y$ are in the x- and y-directions. The superscript (1) and (2) refer to the upper fluid and lower fluid, respectively. The fluid with density $\rho^{(1)}$, uniform velocity $U_0^{(1)}$, porous permeability q_1 and hydrostatic pressure

$$P_0^{(1)} = -\left(\rho^{(1)} g y + \eta^{(1)} U_0^{(1)} q_1^{-1} x + \tfrac{1}{2}\mu^{(1)} \left(H_0^{(1)} + H_{00}^{(1)} \cos \varpi t\right)^2\right), \tag{2}$$

occupies the upper half-space for $y \geq 0$, while the fluid with density $\rho^{(2)}$, uniform velocity $U_0^{(2)}$, porous permeability q_2 and pressure

$$P_0^{(2)} = -\left(\rho^{(2)} g y + \eta^{(2)} U_0^{(2)} q_2^{-1} x + \tfrac{1}{2}\mu^{(2)} \left(H_0^{(2)} + H_{00}^{(2)} \cos \varpi t\right)^2\right), \tag{3}$$

occupies the lower half-space for $y \leq 0$, where g is the gravitational acceleration in the negative $y-$direction. The interface between the fluids is assumed to be well

defined and initially flat and forms the plane $y = 0$. In fact, a sharp interface between the two fluids may not exist. Rather, there is an ill-defined transition region in which the two fluids intermix. The width of this transition zone is usually small compared with the other characteristic length of the motion; hence, for the purpose of the mathematical analysis, we shall assume that the fluids are separated by a sharp interface.

In a magneto-quasi-static system with negligible displacement current, Maxwell's equations in the presence of free electric surface currents are

$$\nabla.\ (\mu^{(j)}\underline{H}^{(j)}(t)) = 0\,, \quad j = 1, 2 \tag{4}$$

$$\nabla \times \underline{H}^{(j)}(t) = \underline{J}_f(t), \tag{5}$$

where the magnetic permeability for the j fluid phase is $\mu^{(j)}$ and $\underline{J}_f(t)$ is the time-dependent surface current vector. It is noted that, In the presence of the free-electric surface currents on the fluid interface, the initial tangential component for the magnetic field could not be continuous across the interface between the fluids, so that $H^{(1)}(t) - H^{(2)}(t) = J_f(t)$. It is convenient to introduce the following equilibrium relations:

$$H_0^{(1)} = \frac{H}{H-1}J_0\,, \text{ and } H_0^{(2)} = \frac{1}{H-1}J_0 \tag{6}$$

where $H$is the stratified magnetic field intensity $H \equiv \frac{H_0^{(1)}}{H_0^{(2)}}$ and J_0 is defined as

$$H_0^{(1)} - H_0^{(2)} = J_0. \tag{7}$$

In accordance with the validity of the quasi-static approximation, a stream function $\psi(x, y, t)$ can be introduced so that the total magnetic field is given by

$$\underline{H}^{(1)}(t) = \left(\frac{\partial\psi^{(1)}}{\partial y} + \frac{H}{H-1}(1 + \varepsilon\,\cos\varpi\, t)J_0\right)\underline{e}_x - \left(\frac{\partial\psi^{(1)}}{\partial x}\right)\underline{e}_y, \tag{8}$$

$$\underline{H}^{(2)}(t) = \left(\frac{\partial\psi^{(2)}}{\partial y} + \frac{1}{H-1}(1 + \varepsilon\,\cos\varpi\, t)J_0\right)\underline{e}_x - \left(\frac{\partial\psi^{(2)}}{\partial x}\right)\underline{e}_y. \tag{9}$$

Clearly, the stream function $\psi(x, y, t)$ guarantees that (5) is satisfied, while the remaining bulk equation ($\nabla\times\underline{H}(t) = 0$) shows that the function ψ satisfies Laplace's equation

$$\nabla^2\phi^{(i)} = 0. \tag{10}$$

It is convenient to insure that $\psi(x,y,t)$ is a finite function presented due to the interface disturbance. Far from the interface its influence is neglected. Therefore both the partial derivative for $\psi(x,y,t)$, with respect to x and y, must vanish as $y \to \pm\,\infty$. In other words, far from the interface, the stream functions are assumed to have

$$\psi^{(1)}(x, +\infty, t) = \psi_\infty^{(1)} \text{ and } \psi^{(2)}(x, -\infty, t) = \psi_\infty^{(2)} \tag{11}$$

where $\psi_\infty^{(1)}$ and $\psi_\infty^{(2)}$ are two different finite constants.

Fluid flow through a porous medium is often given by the phenomenological Darcy equation. Thus, the equations governing two-dimensional motion of an incompressible fluid through porous medium are (see [13], [16] and [34]).

$$\rho\left[\frac{\partial \underline{V}}{\partial t} + (\underline{V}\ .\nabla)\underline{V}\right] = -\nabla P - \rho g \underline{e}_y - \frac{\eta}{q}\underline{V}, \tag{12}$$

associated with the continuity equation

$$\nabla \cdot \underline{V} = 0, \tag{13}$$

where $\underline{V}$ is the fluid velocity vector. The function P refers to the fluid pressure. The parameters ρ, η and q are the fluid density, viscosity and permeability of the medium respectively. The permeability q describes the ability of the fluid to flow through the porous medium.

Introducing the potential velocity $\nabla\phi(x, y, t)$ so that the total fluid velocity is given by

$$\underline{V}^{(j)}(x, y, t) = U_0^{(j)}\, \underline{e}_x - \nabla\phi^{(j)}(x, y, t). \tag{14}$$

Based on the condition of the velocity field be constant at infinity, it follows that the velocity potential tends to constant values as $y \to \pm\,\infty$. This requirement on the potential is expressed as the function $\nabla\phi^{(j)}(x, \pm\infty, t) \to 0$. Expression (14) should be substituted into the above system and an equivalent boundary value problem to solve for the function $\phi(x, y, t)$. This will be obtained later. In view of the continuity equation (13) the following Laplace equation will be imposed:

$$\nabla^2\phi^{(j)}(x, y, t) = 0. \tag{15}$$

Inserting (14) into equation of motion (12) we get

$$\left(\rho^{(j)}\frac{\partial}{\partial t} + \rho^{(j)}U_0^{(j)}\frac{\partial}{\partial x}\eta^{(j)}q_j^{-1}\right)\nabla\phi^{(j)}(x, y, t) =$$

$$\nabla P^{(j)}(x, y, t) + \eta^{(j)}U_0^{(j)}q_j^{-1}\,\underline{e}_x + \rho^{(j)}g\,\underline{e}_y. \tag{16}$$

At the equilibrium state we have $\phi^{(j)} = 0$ and $P^{(j)} = P_0^{(j)}$, hence

$$\frac{\partial P_0^{(j)}}{\partial x} + \eta^{(j)}U_0^{(j)}q_j^{-1} = 0 \text{ and } \frac{\partial P_0^{(j)}}{\partial y} + \rho^{(j)}g = 0 \tag{17}$$

The solutions for these partial differential equations are

$$\pi_0^{(i)}(x, y, t) = -\rho^{(i)}gy - \frac{\eta^{(i)}}{q^{(i)}}V_0^{(i)}x + \lambda_0^{(i)}(x, y, t)\,, \quad i = 1, 2. \tag{18}$$

where $\lambda_0^{(i)}(x, y, t)$ is the constant of integration. The balance of the normal stress tensor at the interface leads to

$$C_0^{(2)} - C_0^{(1)} = \frac{1}{2}\left[\mu^{(1)}(H_0^{(1)} + H_{00}^{(1)}\cos\varpi t)^2 - \mu^{(2)}(H_0^{(2)} + H_{00}^{(2)}\cos\varpi t)^2\right]. \tag{19}$$

It can be noted that the perturbed quantities $\phi(x, y, t)$ and $P(x, y, t)$ are related by

$$P^{(j)}(x, y, t) = \left(\rho^{(j)}\frac{\partial}{\partial t} + \rho^{(j)}U_0^{(j)}\frac{\partial}{\partial x}\eta^{(j)}q_j^{-1}\right)\phi^{(j)}(x, y, t). \tag{20}$$

3. Boundary Conditions

The solutions for the velocity potential $\phi^{(j)}(x,y,t)$ and the magnetic stream function $\psi^{(j)}(x,y,t)$ have to satisfy the boundary conditions, so that, if we assume that the interface between the two fluids is given by $S(x,y,t) = y-\xi(x,t) = 0$, the linearized boundary conditions at the interface $y = \xi(x,t)$ are listed below ([9] and [35]):

(i) At the surface of separation, the physical conditions to be satisfied for the stress are that the tangential component is zero and the normal one is discontinuous under the influence of the surface tension (Batchelor [36]). Therefore, the normal component of the stress tensor σ_{ij} is related to the surface tension by [37]

$$\left(\sigma_{jy}^{(1)} - \sigma_{jy}^{(2)}\right) n_y = -n_j \sigma_T \ \nabla^2 \xi, \quad y = \xi, \tag{21}$$

where σ_T is the surface tension coefficient, n_x and n_y are, respectively, the horizontal and vertical components for the unit normal vector $\underline{n}$ to the interface, in which

$$\underline{n} = \frac{\nabla s}{|\nabla s|}. \tag{22}$$

The stress tensor $\sigma_{ij}$is given by

$$\sigma_{ij} = -P\delta_{ij} + \mu H_i H_j - \tfrac{1}{2}\mu H^2 \delta_{ij} + \eta\left(\tfrac{\partial V_i}{\partial x_j} + \tfrac{\partial V_j}{\partial x_i}\right), \tag{23}$$

where δ_{ij} is the Kronecker's delta.

(ii) An equation expressing the assumed material character of the dividing surface is required. Such an equation is

$$\frac{\partial \xi}{\partial t} = -\frac{\partial \phi^{(j)}}{\partial y} - \frac{\partial \xi}{\partial x} U_0^{(j)}, \quad j = 1,2, \quad y = \xi, \tag{24}$$

where U_0 is the equilibrium horizontal velocity.

(iii) The continuity of the normal component of the magnetic displacement at the surface of separation.

$$\underline{n} \ \cdot \ \left(\mu^{(1)} \underline{H}^{(1)}(t) - \mu^{(2)} \underline{H}^{(2)}(t)\right) = 0, \quad y = \xi. \tag{25}$$

(iv) Owing to the presence of free electric surface currents on the interface, the tangential component of the magnetic field is discontinuous. At this end, we are in need to use another boundary condition instead of this condition. Therefore the continuity of the tangential stress is used (Melcher [9]). This requires

$$\left(\sigma_{xy}^{(1)} - \sigma_{xy}^{(2)}\right) n_y + \left(\sigma_{xx}^{(1)} - \sigma_{xx}^{(2)}\right) n_x = 0, \quad y = \xi. \tag{26}$$

Thus, the appropriate magnetic boundary conditions here are reduced, respectively, to

$$\frac{\partial \xi}{\partial x} \frac{1}{H-1}\left(\mu^{(1)} H - \mu^{(2)}\right)\left(J_0 + J_{00}\cos \varpi\, t\right) + \left(\mu^{(1)} \frac{\partial \psi^{(1)}}{\partial x} - \mu^{(2)} \frac{\partial \psi^{(2)}}{\partial x}\right) = 0,$$

$$y = 0\,, \tag{27}$$

$$\begin{aligned}\left(\mu^{(1)} H \frac{\partial \psi^{(1)}}{\partial x} - \mu^{(2)} \frac{\partial \psi^{(2)}}{\partial x}\right) \frac{1}{H-1} \left(J_0 + J_{00}\cos\varpi\, t\right) + \\ \frac{\partial \xi}{\partial x}\left(\mu^{(1)} H^2 - \mu^{(2)}\right) \frac{1}{(H-1)^2} \left(J_0 + J_{00}\cos\varpi\, t\right)^2 + \\ 2\frac{\partial^2}{\partial x \partial y}\left(\eta^{(1)}\phi^{(1)} - \eta^{(2)}\phi^{(2)}\right) \quad = \quad 0\,,\end{aligned} \tag{28}$$

The above boundary conditions represented here are prescribed at the interface $y = \xi(x,t)$. As the interface is deformed all variables are slightly perturbed from their equilibrium values. Because the interfacial displacement is small, the boundary conditions on perturbation interfacial variables need to be evaluated at the equilibrium position rather than at the interface. Therefore, it is necessary to express all the physical quantities involved in terms of Maclaurin series about $y = 0$.

4. Linear Perturbation and derivation of the Characteristic Equation

To perform a linear stability analysis, the interface is perturbed by a sinusoidal wave of small amplitude,

$$\xi(x,t) = \gamma(t)\, e^{ikx}, \tag{29}$$

where the wavenumber k is assumed to be real and positive, $i = \sqrt{-1}$ and γ is an arbitrary function of time, which determines the behaviour of the amplitude of the disturbance of the interface. Perturbation bulk variables are functions of both the horizontal and vertical coordinates as well as time. The deformation in the interface $y = 0$ is due to the perturbation about the equilibrium values for all the other variables. The equations of motion and the boundary conditions mentioned previously will be solved for these perturbations under the assumption that the perturbations are small, that is, all equations of motion and boundary conditions will be linearized in the perturbed quantities. The form of the horizontal variation for all the other perturbed variables will be the same as the displacement description (29).

In accordance with the interface deflecting given by (29) and in view of a standard Fourier decomposition, we may similarly assume that the bulk solutions are of the form

$$\phi^{(j)}(x,y,t) = \hat{\phi}^{(j)}(y,t) e^{ikx}, \tag{30}$$

$$P^{(j)}(x,y,t) = \hat{P}^{(j)}(y,t) e^{ikx}, \tag{31}$$

$$\psi^{(j)}(x,y,t) = \hat{\psi}^{(j)}(y,t) e^{ikx}. \tag{32}$$

As is customary in hydrodynamic stability analysis [1], we insert (30) into Laplace equation (15), the resulting solutions in view of the boundary condition (25) yield

$$\phi^{(1)}(x,y,t) = \frac{1}{k}\left(\frac{d\gamma}{dt} + ikU_0^{(1)}\gamma\right) e^{ikx-ky}\,, \quad y > 0\,, \tag{33}$$

$$\phi^{(2)}(x,y,t) = -\frac{1}{k}\left(\frac{d\gamma}{dt} + ikU_0^{(2)}\gamma\right) e^{ikx+ky}\,, \quad y < 0\,. \tag{34}$$

Inserting (33) and (34) into (20), accordingly, the pressure distribution in the two fluid phases is

$$\begin{aligned} P^{(1)}(x,y,t) &= \frac{1}{k}\left[\rho^{(1)}\frac{d^2\gamma}{dt^2}+\left(2ik\rho^{(1)}U_0^{(1)}+\eta^{(1)}q_1^{-1}\right)\frac{d\gamma}{dt}+\right. \\ &\left. kU_0^{(1)}\left(i\eta^{(1)}q_1^{-1}-k\rho^{(1)}U_0^{(1)}\right)\gamma\right]e^{ikx-ky}, \\ &y>0\,, \end{aligned} \tag{35}$$

$$\begin{aligned} P^{(2)}(x,y,t) = -\frac{1}{k}&\left[\rho^{(2)}\frac{d^2\gamma}{dt^2}+\left(2ik\rho^{(2)}U_0^{(2)}+\eta^{(2)}q_2^{-1}\right)\frac{d\gamma}{dt}+\right. \\ &\left. kU_0^{(2)}\left(i\eta^{(2)}q_2^{-1}-k\rho^{(2)}U_0^{(2)}\right)\gamma\right]e^{ikx+ky}, \\ &y<0\,. \end{aligned} \tag{36}$$

Substituting (32) into Laplace equation (10), the resulting solution in view of the above boundary conditions (27) and (28) gives

$$\begin{aligned} \psi^{(1)}(x,y,t) &= \frac{1}{\mu^{(1)}\left(J_0+J_{00}\cos\varpi\, t\right)}\left\{2\left(\eta^{(1)}-\eta^{(2)}\right)\frac{d\gamma}{dt}+\right. \\ &\left[2ik\left(\eta^{(1)}U_0^{(1)}-\eta^{(2)}U_0^{(2)}\right)-\right. \\ &\left.\left.\frac{\mu^{(1)}H}{H-1}\left(J_0+J_{00}\cos\varpi\, t\right)^2\right]\gamma\right\}e^{ikx-ky} \end{aligned} \tag{37}$$

$$\begin{aligned} \psi^{(2)}(x,y,t) &= \frac{1}{\mu^{(2)}\left(J_0+J_{00}\cos\varpi\, t\right)}\left\{2\left(\eta^{(1)}-\eta^{(2)}\right)\frac{d\gamma}{dt}+\right. \\ &\left[2ik\left(\eta^{(1)}U_0^{(1)}-\eta^{(2)}U_0^{(2)}\right)-\right. \\ &\left.\left.\frac{\mu^{(2)}}{H-1}\left(J_0+J_{00}\cos\varpi\, t\right)^2\right]\gamma\right\}e^{ikx+ky} \end{aligned} \tag{38}$$

In what follows we shall derive the characteristic equation governing the interfacial waves. Inserting (33)–(38) into the normal stress tensor (21), to replace the dependent on the potential velocity $\phi^{(j)}$, the magnetic stream function $\psi^{(j)}$ and the fluid pressure function $P^{(j)}$ by their dependent on the amplitude $\gamma(t)$, finally we obtain

$$\begin{aligned} (\rho^{(1)}+\rho^{(2)})\frac{d^2\gamma}{dt^2}+&\left[\left(\frac{-4k^2}{H-1}+q_1^{-1}\right)\eta^{(1)}+\left(4k^2\frac{H}{H-1}+q_2^{-1}\right)\eta^{(2)}+\right. \\ &\left.2ik\left(\rho^{(1)}U_0^{(1)}+\rho^{(2)}U_0^{(2)}\right)\right]\frac{d\gamma}{dt}+\left[k^3\sigma_T-kg(\rho^{(1)}-\rho^{(2)})-\right. \\ &k^2\left(\rho^{(1)}{U_0^{(1)}}^2+\rho^{(2)}{U_0^{(2)}}^2\right)+ik\left(\frac{-4k^2}{H-1}+q_1^{-1}\right)U_0^{(1)}\eta^{(1)}+ \\ &ik\left(4k^2\frac{H}{H-1}+q_2^{-1}\right)U_0^{(2)}\eta^{(2)}+ \\ &\left.\frac{k^2}{(H-1)^2}\left(\mu^{(1)}H^2+\mu^{(2)}\right)\left(J_0+J_{00}\cos\,\varpi t\right)^2\right]\gamma = 0\,. \end{aligned} \tag{39}$$

Equation (39) is a complicated damped Mathieu equation. In which complex coefficients are included. This equation represents the dispersion equation which governs the amplitude of the surface waves propagating between two moving Darcian fluids. This equation has a growth rate solution, the stability analysis being rather complex. To economize this complexity, a mathematical simplification is useful here to overcome the complexity. This simplification will be based on the assumption that the fluids have weak viscous effects. In dealing with the periodic solutions of the Mathieu's equation (39), a stability analysis can be performed using the marginal state treatment. Marginal stability holds trivially in the inviscid case. To obtain the marginal state for moving viscous flow, a reduced form of the Mathieu equation (39) is needed.

5. Stability Analysis in View of Weak Viscous Effect

In the light of weak viscous effects, the complex equation (39) can be put in a reduction form. This can be accomplished in the following manner.

Owing to the properties of the viscous problem considered here in which the viscous problem is regarded as a slightly departure from the inviscid case, we can easily verify that $(\eta = \delta\hat{\eta})$, then the above system has the form $\alpha + \delta\,\beta = 0$; where α refers to the inviscid problem, in which it is regarded as a function of the fluid density $\rho^{(j)}$, the fluid velocity $U_0^{(j)}$, magnetic force and the term β refers to viscous contributions, in which it is a function of the fluid viscosity $\eta^{(j)}$ and porous permeability q_j. The artificial parameter δ is a small dimensionless quantity, which measures viscosity. Owing to linearly independence in δ we have $\alpha = 0$ and $\beta = 0$. According to this fact, the system (39) will be separated, respectively, into the following two parts:

$$\begin{aligned}\left(\rho^{(1)}+\rho^{(2)}\right)\frac{d^2\gamma}{dt^2}+\left[2ik\left(\rho^{(1)}U_0^{(1)}+\rho^{(2)}U_0^{(2)}\right)\frac{d\gamma}{dt}+\right.\\ \left[k^3\sigma_T-kg\left(\rho^{(1)}-\rho^{(2)}\right)-k^2\left(\rho^{(1)}{U_0^{(1)}}^2+\rho^{(2)}{U_0^{(2)}}^2\right)+\right.\\ \left.\left.\frac{k^2}{(H-1)^2}\left(\mu^{(1)}H^2+\mu^{(2)}\right)\left(J_0+J_{00}\cos\,\varpi t\right)^2\right]\gamma &= 0\,, \qquad (40)\end{aligned}$$

$$\begin{aligned}\left[\left(\frac{-4k^2}{H-1}+q_1^{-1}\right)\hat{\eta}^{(1)}+\left(\frac{4k^2H}{H-1}+q_2^{-1}\right)\hat{\eta}^{(2)}\right]\frac{d\gamma}{dt}+\\ ik\left[\left(\frac{-4k^2}{H-1}+q_1^{-1}\right)U_0^{(1)}\hat{\eta}^{(1)}\;+\left(\frac{4k^2H}{H-1}+q_2^{-1}\right)U_0^{(2)}\hat{\eta}^{(2)}\right]\gamma &= 0\,. \qquad (41)\end{aligned}$$

Equation (40) refers to the behaviour of the wave propagation between two inviscid fluids in the presence of free electric surface currents. In the other side, equation (31) represents the viscous correction of the inviscid fluids. Combining these equations yields the following Mathieu equation:

$$\frac{d^2\gamma(t)}{d\,t^2}+\left[\omega^2+Q\left(J_0+J_{00}\cos\varpi\,t\right)^2\right]\gamma(t)=0\,, \qquad (42)$$

where

$$Q = \frac{k^2\left(\mu^{(1)}H^2 + \mu^{(2)}\right)}{(H-1)^2(\rho^{(1)}+\rho^{(2)})}\,,$$

$$\begin{aligned}\omega^2 \;=\; & \frac{1}{(\rho^{(1)}+\rho^{(2)})}\left\{ k^3\sigma_T \,- kg(\rho^{(1)}-\rho^{(2)}) - k^2\left(\rho^{(1)}{U_0^{(1)}}^2 + \rho^{(2)}{U_0^{(2)}}^2\right) + \right.\\ & 2k^2\left(\rho^{(1)}U_0^{(1)} + \rho^{(2)}U_0^{(2)}\right)\left[\frac{4k^2}{H-1}\left(\eta^{(2)}U_0^{(2)}H - \eta^{(1)}U_0^{(1)}\right) + \right.\\ & \left.\left(\eta^{(1)}U_0^{(1)}q_1^{-1} + \eta^{(2)}U_0^{(2)}q_2^{-1}\right)\right]\times\\ & \left.\left[\frac{4k^2}{H-1}\left(\eta^{(2)}H - \eta^{(1)}\right) + \left(\eta^{(1)}q_1^{-1} + \eta^{(2)}q_2^{-1}\right)\right]^{-1}\right\} \end{aligned} \tag{43}$$

It should be noticed that equation (42) represents the Mathieu equation without the viscous damping term. The viscosity is included in the coefficient ω^2 for the variable $\gamma(t)$ and should affect the stability behaviour. Here, one can notice that equation (43) represents the dispersion relation that is satisfied in the absence of the applied magnetic fields. Clearly, a singularity occurs owing to the vanishing of the dominator of ω^2. This singularity arises at a critical value of the stratified magnetic field H_c given by

$$H_C = \frac{(4k^2 + q_1^{-1})\eta + q_2^{-1}}{(4k^2 + q_2^{-1}) + \eta q_1^{-1}}\,, \tag{44}$$

where η is the stratified viscosity $\eta = \frac{\eta^{(1)}}{\eta^{(2)}}$. This is the relation between the stratified magnetic field and the stratified viscosity.

If the critical value H_C is excluded, the wave train solution for the static magnetic field can be achieved. This can be accomplished when the term $\omega^2 + QJ_0^2$ is positive. Thus, we need

$$\begin{aligned} J_0^2 > J^* \;=\; & \frac{(H-1)^2}{k^2\left(\mu^{(1)}H^2 + \mu^{(2)}\right)}\left\{ kg\left(\rho^{(1)}-\rho^{(2)}\right) - k^3\sigma_T + \right.\\ & k^2\left(\rho^{(1)}{U_0^{(1)}}^2 + \rho^{(2)}{U_0^{(2)}}^2\right) - 2k^2\left(\rho^{(1)}U_0^{(1)} + \rho^{(2)}U_0^{(2)}\right)\times\\ & \left[\frac{4k^2}{H-1}\left(\eta^{(2)}U_0^{(2)}H - \eta^{(1)}U_0^{(1)}\right) + \left(\eta^{(1)}U_0^{(1)}q_1^{-1} + \eta^{(2)}U_0^{(2)}q_2^{-1}\right)\right]\times\\ & \left.\left[\frac{4k^2}{H-1}\left(\eta^{(2)}H - \eta^{(1)}\right) + \left(\eta^{(1)}q_1^{-1} + \eta^{(2)}q_2^{-1}\right)\right]^{-1}\right\} > 0\,. \end{aligned} \tag{45}$$

Another dramatic aspect of the stability behaviour can be found when the field frequency ϖ is presented. In dealing with the case of oscillating the magnetic field, we assume that the static part J_0 has a zero value. At this stage, stability occurs whence the following inequality is satisfied [38]:

$$J_{00}^4Q^2 + 16(\varpi^2 - \omega^2)QJ_{00}^2 + 32\omega^2(\varpi^2 - \omega^2) > 0\,. \tag{46}$$

Namely

$$(J_{00}^2 - J_1^*)(J_{00}^2 - J_2^*) > 0\,, \tag{47}$$

where

$$J_{1,2}^* = \frac{8}{Q}\left[-(\varpi^2 - \omega^2) \pm \sqrt{(\varpi^2 - \omega^2)(\varpi^2 - \tfrac{3}{2}\omega^2)}\right]. \tag{48}$$

This stability criterion reduces to the problem of the bounded regions of the Mathieu functions, as given in [39]. The transition curves J_1^* and J_2^* should start from the point $H = 1$ and from the point satisfying $\varpi^2 = \omega^2$, which represents the resonance point. There exists another starting point satisfying $\omega^2 = 0$. Therefore, in the (J_{00}^2, H)-plane, the transition curves will intersect the H-axis at three points, given by $H_1 = 1$,

$$\begin{aligned} H_2 \;=\; & \left[k^2\sigma_T - g\left(\rho^{(1)} - \rho^{(2)}\right) - \varpi^2\left(\rho^{(1)} + \rho^{(2)}\right) - k\left(\rho^{(1)}{U_0^{(1)}}^2 + \rho^{(2)}{U_0^{(2)}}^2\right)\right] \times \\ & \left[\left(4k^2 + q_1^{-1}\right)\eta + q_2^{-1}\right] + 2k\left(\rho^{(1)}U_0^{(1)} + \rho^{(2)}U_0^{(2)}\right) \times \\ & \left[\left(4k^2 + q_1^{-1}\right)\eta U_0^{(1)} + U_0^{(2)}q_2^{-1}\right] \times \\ & \left\{\left[k^2\sigma_T - g(\rho^{(1)} - \rho^{(2)}) - \varpi^2(\rho^{(1)} + \rho^{(2)}) - k\left(\rho^{(1)}{U_0^{(1)}}^2 + \rho^{(2)}{U_0^{(2)}}^2\right)\right] \times \right. \\ & \left[\left(4k^2 + q_2^{-1}\right) + \eta q_1^{-1}\right] + \\ & \left. 2k\left(\rho^{(1)}U_0^{(1)} + \rho^{(2)}U_0^{(2)}\right)\left[\left(4k^2 + q_2^{-1}\right)U_0^{(2)} + \eta U_0^{(1)}q_1^{-1}\right]\right\}^{-1}, \end{aligned} \tag{49}$$

$$\begin{aligned} H_3 \;=\; & \left\{\left[k^2\sigma_T - g(\rho^{(1)} - \rho^{(2)}) - k\left(\rho^{(1)}{U_0^{(1)}}^2 + \rho^{(2)}{U_0^{(2)}}^2\right)\right]\right. \\ & \left[\left(4k^2 + q_1^{-1}\right)\eta + q_2^{-1}\right] + 2k\left(\rho^{(1)}U_0^{(1)} + \rho^{(2)}U_0^{(2)}\right) \times \\ & \left.\left[\left(4k^2 + q_1^{-1}\right)\eta U_0^{(1)} + U_0^{(2)}q_2^{-1}\right]\right\} \times \\ & \left\{\left[k^2\sigma_T - g\left(\rho^{(1)} - \rho^{(2)}\right) - k\left(\rho^{(1)}{U_0^{(1)}}^2 + \rho^{(2)}{U_0^{(2)}}^2\right)\right]\right. \\ & \left[\left(4k^2 + q_2^{-1}\right) + \eta q_1^{-1}\right] + 2k\left(\rho^{(1)}U_0^{(1)} + \rho^{(2)}U_0^{(2)}\right) \times \\ & \left.\left[\left(4k^2 + q_2^{-1}\right)U_0^{(2)} + \eta U_0^{(1)}q_1^{-1}\right]\right\}^{-1}. \end{aligned} \tag{50}$$

It is well known that free electric surface currents density disappear from the fluid interface whence the stratified magnetic field has the exact unit value. From the above calculations one can found that the free electric surface currents density will disappear from the interface at another two values for the stratified magnetic field, namely H_2 and H_3. These two values have not been found in the case of the absence of the field frequency ϖ.

5.1. *Stability Diagram and Numerical Estimation*

In graphing the stability picture at this scope, numerical estimation is made for the stability condition (45), in the static case, and the stability criteria (46) to assess

the implications of the field frequency. Therefore, calculations are done for the transition curves J^* and $J^*_{1,2}$. Before going into the details of these calculations, it is convenient to seek all the physical parameters in non-dimensional form. We introduce the characteristic length L of order $\left(\frac{\eta^{(2)\,2}}{\rho^{(2)^2}g}\right)^{\frac{1}{3}}$ and the characteristic time T of order $\left(\frac{\eta^{(2)}}{\rho^{(2)}g^2}\right)^{\frac{1}{3}}$. Other dimensionless quantities are given by

$$k = \frac{k^*}{L}\,, \quad q_j = q_j^* L^2\,, \quad \sigma_T = \sigma_T^* \left(\rho^{(2)} g L^2\right)\,, \quad U_0^{(j)} = U_0^{*(j)} \frac{L}{T}$$

and

$$J(t) = J^*(t) \sqrt{\frac{L\rho^{(2)} g}{\mu^{(2)}}}\,.$$

The superposed $*$ will be omitted later for simplicity and $\rho = \frac{\rho^{(1)}}{\rho^{(2)}}$, $\eta = \frac{\eta^{(1)}}{\eta^{(2)}}$ are used.

The stability diagram that displayed in Figure 1 is made by a plot of transition curve J^* according (45). The electric surface current coefficient J_0^2 is plotted as a function of the stratified magnetic field H. The graph of the plane $(J_0^2 - H)$ refers to a stable zone characterized by the symbol S bounded by two unstable regions which are characterised by the symbol U. The stable zone starts from the point H=1. At the exact H =1, the stratified field plays a stabilizing role in the absence of J_0^2. A destabilizing influence of the field appears in the neighbourhood of $H = 1$. This stabilizing influence increases as J_0^2 increases. This shows the stabilizing influence of the presence of J_0^2 in the neighbourhood of $H = 1$.

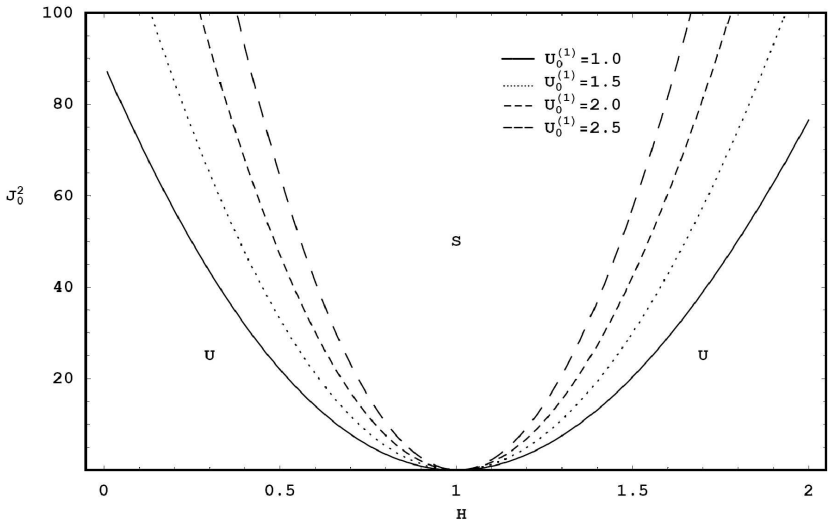

Figure 1 Influence of variation of the velocity $U_0^{(1)}$ on the stability diagram. The graph is for J_0^2 versus H. The graph construction is based on condition (45). The calculations are made for the system having $k = 0.1, \rho = 1.2, \eta = 1.2, \mu = 0.04, q_1^{-1} = 1, q_2^{-1} = 1$ and $\sigma_T = 12$

The stability examination, for the influence of the fluid velocity is included in the present graph in which some curves are drawing to variation of $U_0^{(1)}$, at fixing the velocity $U_0^{(2)}$. Inspection of the stability diagram reveals that the increase in the upper velocity has contracted the width of the stable zone. The same conclusion can be found if we fixe the upper velocity $U_0^{(1)}$ while the lower velocity $U_0^{(2)}$ has some variation. These calculations show that the increase in the fluid velocities plays a destabilizing role.

The effect of the viscosity ratio η, in the presence of free electric surface currents, is shown in Figure 2a) for $U_0^{(1)} > U_0^{(2)}$ and in Figure 2b) where $U_0^{(1)} < U_0^{(2)}$. In Figure 2a), the increase in the viscosity ratio η has contracted the width of the stable zone. Similar behaviour is observed for increasing the parameter q_1^{-1} as shown in Figure 3a). In the other side, in Figure (2-b), the increase in η leads to an increase in the width of the stable zone. Similar effects appear for increasing q_1^{-1} as illustrated in Figure 3b). Therefore, there are two different conclusions for increasing the viscosity parameter η and the permeability parameter, a destabilizing influence for $U_0^{(1)} > U_0^{(2)}$ and a stabilizing effect for $U_0^{(1)} < U_0^{(2)}$. This conclusion has not been observed before.

To screen the influence of the field frequency ϖ on the stability criteria, numerical estimation has been carried out for the transition curves J_1^* and J_2^* according to (36). The results of the calculation are displayed in Figures 4–8. The stability diagram for this calculation has been displayed in the plane $(J_{00}^2 - H)$. In this plane two stable regions S_0 and $S_\varpi$lie between three unstable regions U. The first stable zone S_0 starts from the point$H$ =1. It can be recognized that the stable zone S_0 correspond to the stable zone appearing in Figure 1 and Figure 2a) and b), in the absence of the field frequency. The second stable region S_ϖ is due to the presence of the field frequency ϖ. This stable region lies between the two points H_2 and H_3. The presence of this region indicates the stabilizing role of oscillating the magnetic field. It appears from the stability diagram that an increase in J_{00}^2 leads to an increase in the size of this stable region, so that the stratified magnetic field is more strongly stabilizing in the presence of the electric free surface currents. In the absence of J_{00}^2, as shown in Figures 4–7, the stratified field plays a destabilizing role for $H > H_2(\varpi)$. Inspection of these graphs show that there is a singularity for the transition curves. A major instability arises when $H = H_C$, which lies between the two stable regions S_0 and S_ϖ. In this graph, the critical value of the stratified magnetic field is $H_C = 1.1290323$. The occurrence of this singularity is dependent on the stratified viscosity η, the porous permeability q_j^{-1} and the wavenumber k, while it is independent of both fluid velocity and the field frequency. Very much larger values of the electric surface currents are required to suppress this unstable case. The presence of electric surface currents has constrained this destabilizing role. In contrast with the stable region S_0, the stable region S_ϖ is depending on the field frequency ϖ.

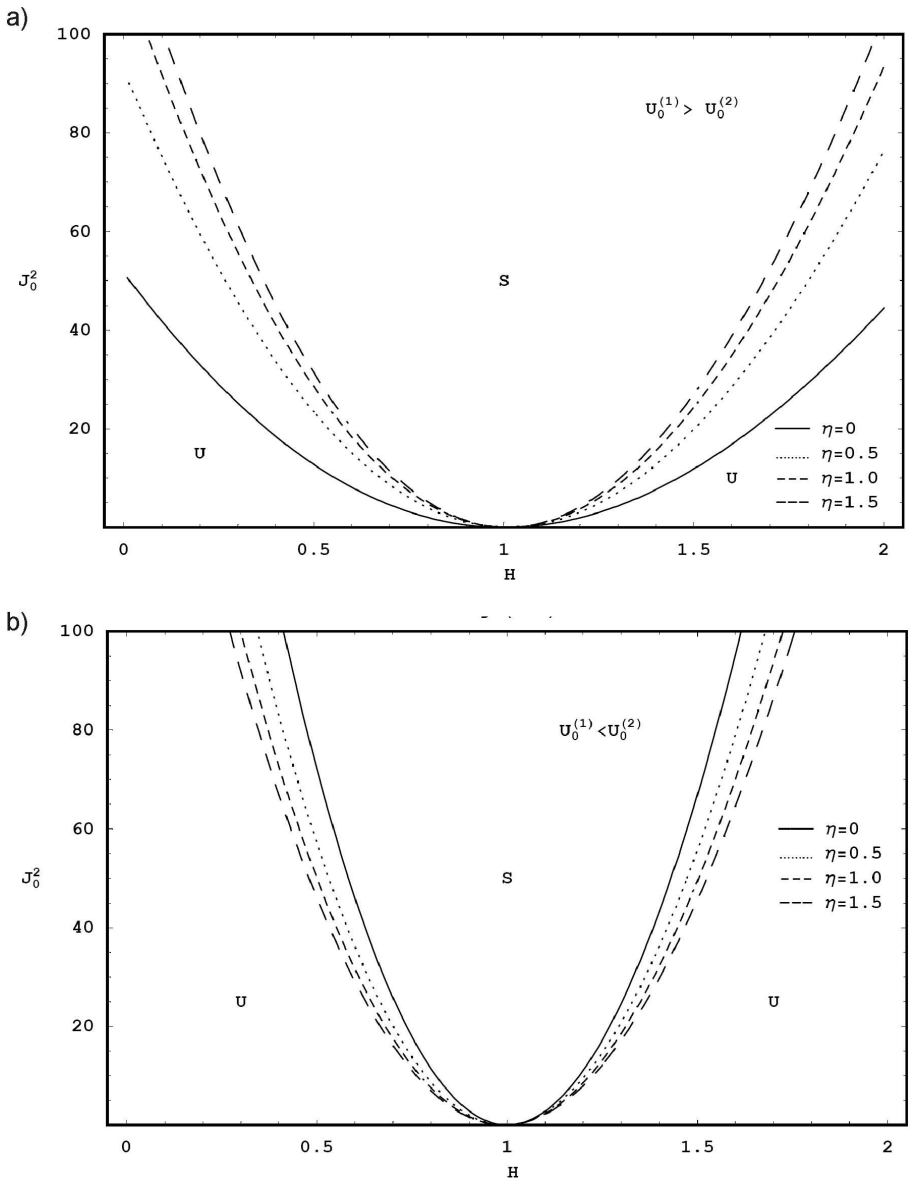

Figure 2 a): Influence of the viscosity ratio on the stability picture for the same system as in Fig. 1, where $\rho = 0.5, U_0^{(1)} = 3$ and $U_0^{(2)} = 1$; b): the same as in Fig. 2a), but $U_0^{(1)} = 1$ and $U_0^{(2)} = 3$

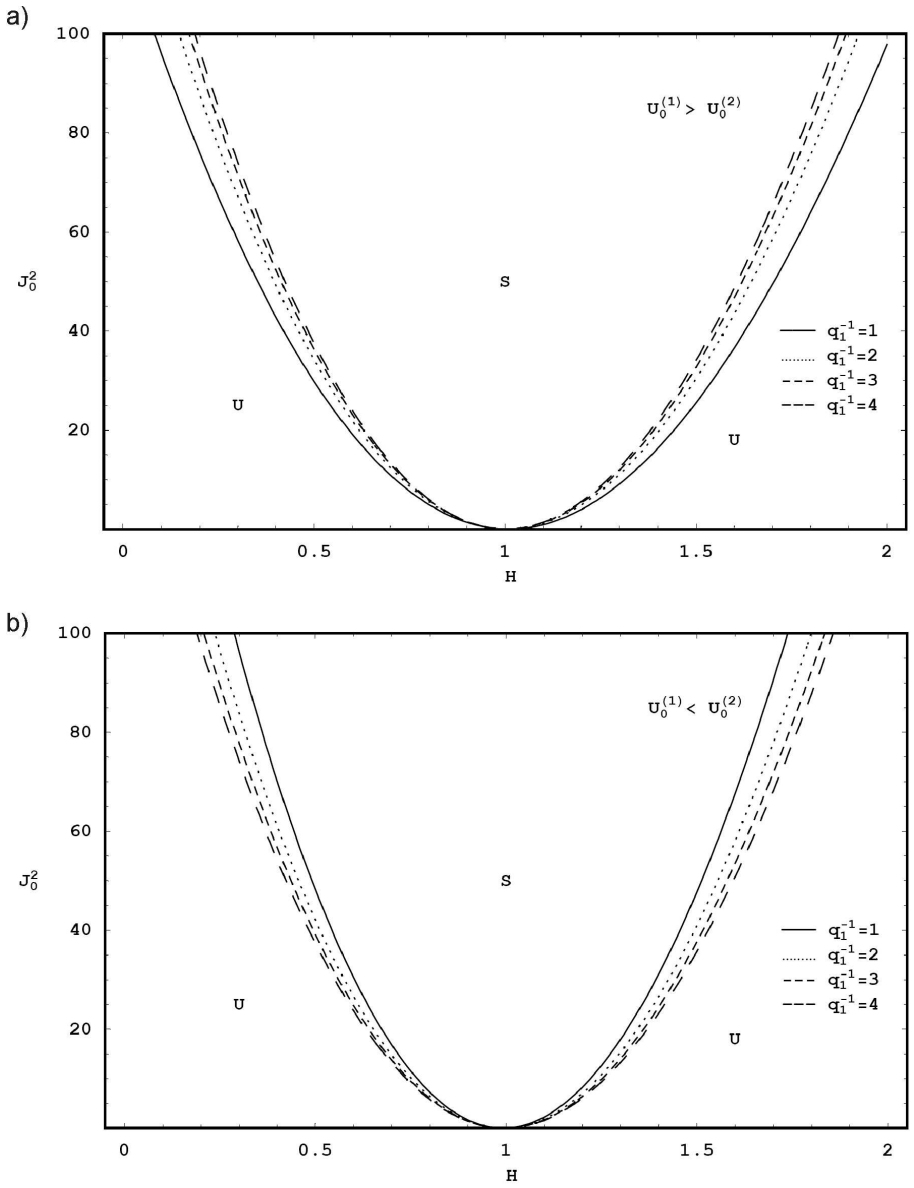

Figure 3 a): Influence of the variation of the porous permeability parameter for the same system as in Fig. 2a), but $\eta = 1.2$; b): for the same system as in Fig. 2b)

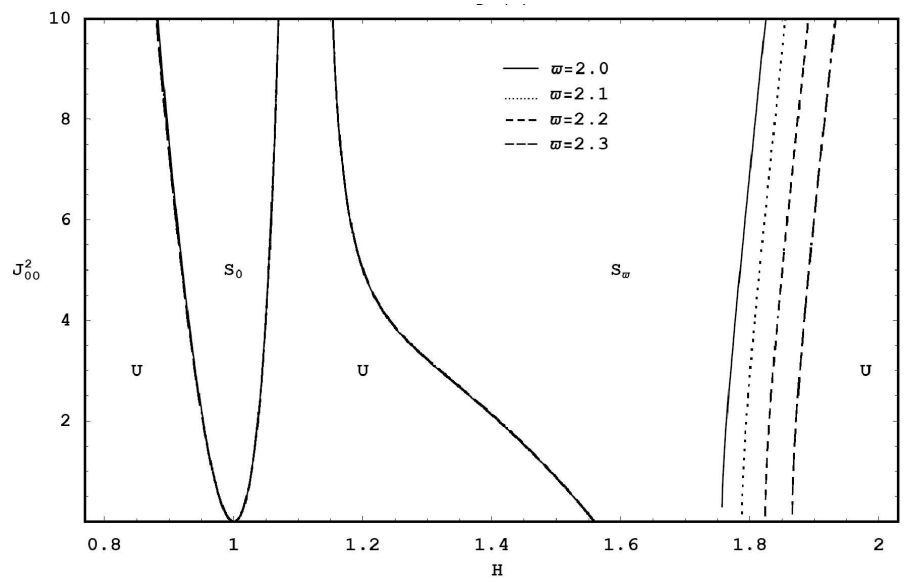

Figure 4 Influence of the field frequency ϖ on the stability behavior. The calculations are made for the stability condition (46) for the system having $k = 1, \rho = 0.7, \eta = 1.2, \mu = 0.4, \varpi = 2$, $q_1^{-1} = 1, q_2^{-1} = 1, U_0^{(1)} = 3, U_0^{(2)} = 1$ and $\sigma_T = 20$

Examination of increasing the field frequency has been displayed in Figure 4. Inspection of this graph shows that an increase in the frequency ϖ increases the size of stable region S_ϖ and shifts it into the direction of increasing H. Thus conclude that the presence as well as the increase of the field frequency plays a stabilizing role in the stability behaviour.

The influence of the increase of fluid velocity $U_0^{(1)}$ on the stability behaviour in the presence of the frequency ϖ is displayed in Figure 5. The graph shown in the plane $(J_{00}^2 - H)$ represents four consequent values of $U_0^{(1)}$ with fixing the lower velocity $U_0^{(2)}$ to unit value so that $U_0^{(1)} > U_0^{(2)}$. It is shown that the increase of the upper velocity leads to a very small decrease in the region S_0 and an increase in the stable region S_ϖ associates with a shift towards the direction of increasing H. This conclusion has not been found in the absence of the frequency ϖ. Now, we have two roles for increasing $U_0^{(1)}$ in the stability picture. These roles are a very small destabilizing effect in the region S_0 and a stabilizing influence in the stable region

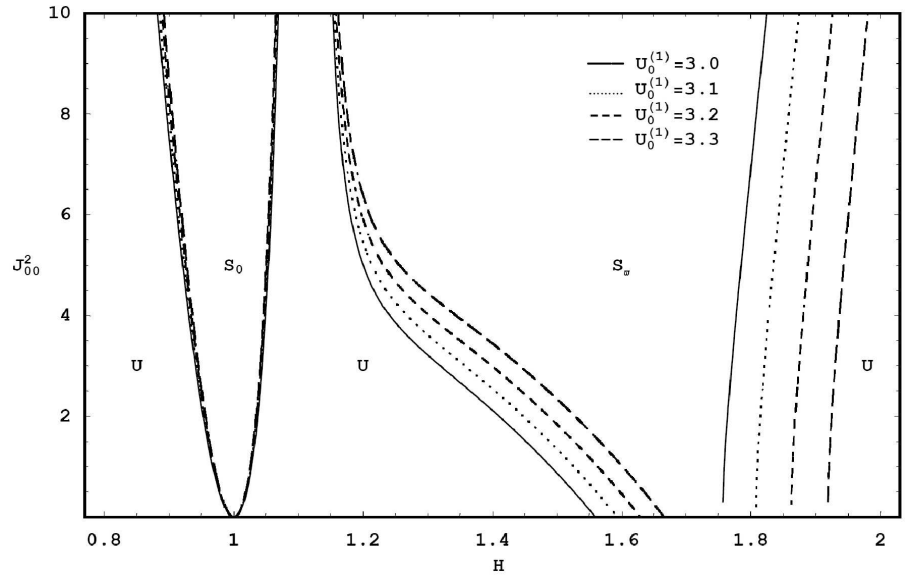

Figure 5 For the same system as in Fig. 4 where $\varpi = 2$

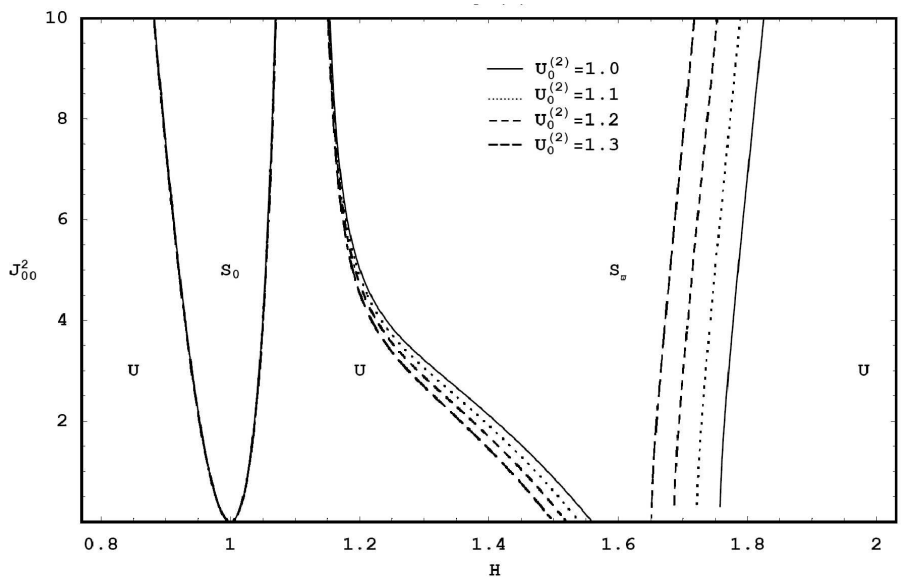

Figure 6 For the same system as in Fig. 5

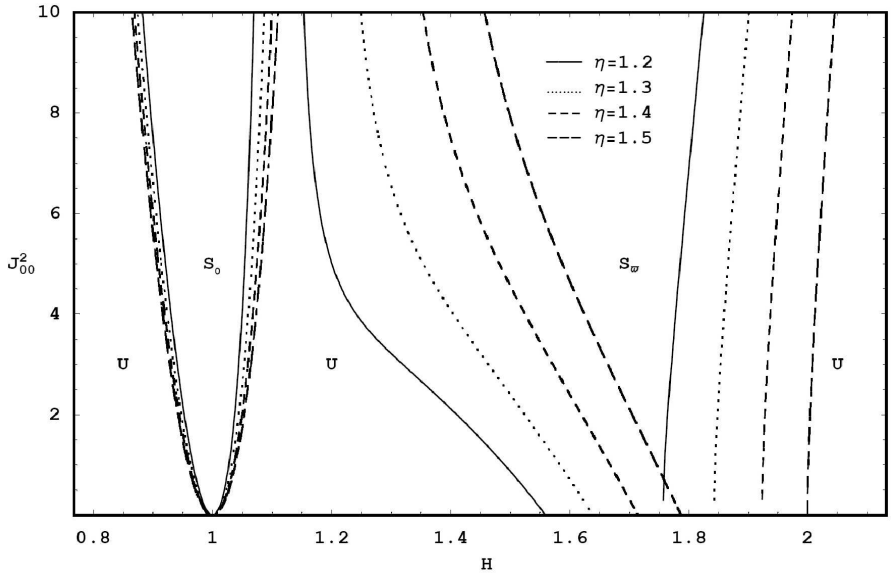

Figure 7 For the same system as in Fig. 5

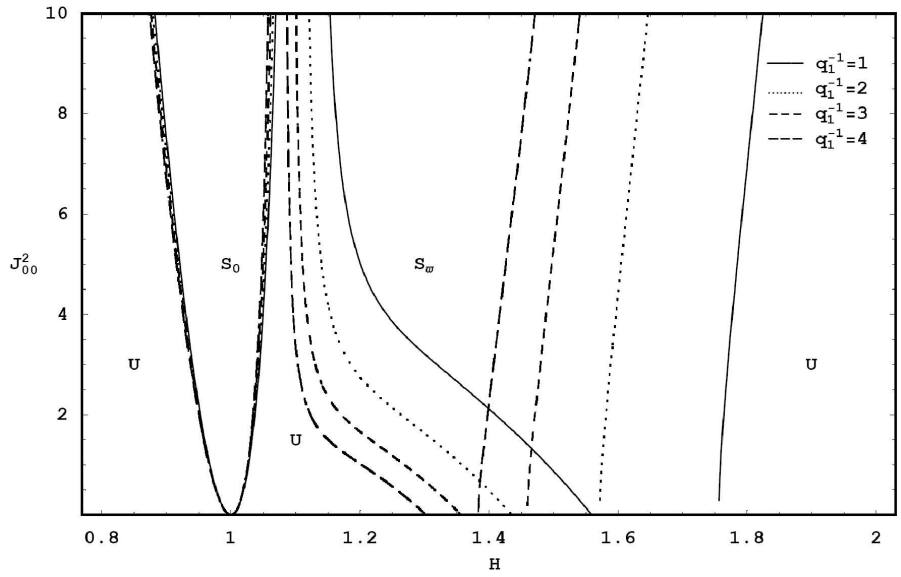

Figure 8 For the same system as in Fig. 5

S_{ϖ}. This phenomenon is known as the dual role in the stability behaviour. When the lower velocity $U_0^{(2)}$ has increased under the condition $U_0^{(1)} > U_0^{(2)}$ a destabilizing influence is found as shown in Figure 6.

The examination of increasing the stratified viscosity on the stability picture has been illustrated in Figure 6. Four consequent values for η are used for the sake of investigation. As η is increased the width of the stable area S_0 increases, while the width of the stable S_{ϖ} contracts in width. Thus, two different roles are found for increasing η, a stabilizing influence in the region labeled by S_0 and a destabilizing effect appears in the region of S_{ϖ} associated with small shift towards the direction of increasing H. Therefore the viscosity parameter plays a dual role in the stability criteria in the presence of the field frequency ϖ.

Some variation of the porous permeabilities is assumed in the presence of oscillating the magnetic field. Numerical results are displayed in Figure 7 for four consequent values of q_1^{-1} with fixing q_2^{-1} to the unit value. Inspection of the graph reveals that as the porous permeability q_1^{-1} has been increased the stable area S_{ϖ} shifts to the direction of decreasing the axis-H associated with a contraction in the width. The same observation is found when q_2^{-1} increase instead of q_1^{-1}. This means that the decrease in q_j plays a destabilizing influence. This shows that the increase in the resistance force $(\eta^{(j)}/q_j)$ plays a destabilizing influence in the stability behaviour under the influence of the periodic magnetic field in the presence of free electric surface currents.

6. Alternative Scope for Marginal Stability Analysis

In this section we shall discuss another profile for the marginal stability. Before discussing the stability analysis in the present case, it is convenient to eliminate the imaginary damping terms from the original Mathieu equation (39) by making use of the following transformation:

$$\gamma(t) = \Theta(t) \exp\left[-\frac{ik\left(\rho U_0^{(1)} + U_0^{(2)}\right) t}{\rho + 1}\right]. \tag{51}$$

Then equation (39) reduces to

$$\frac{d^2\Theta}{dt^2} + A\frac{d\Theta}{dt} + \left[\Omega^2 + i\lambda + Q\left(J_0 + J_{00}\cos\varpi\, t\right)^2\right]\Theta = 0, \tag{52}$$

where

$$A = \frac{1}{\rho+1}\left[\left(\frac{-4k^2}{H-1} + q_1^{-1}\right)\eta + \left(4k^2\frac{H}{H-1} + q_2^{-1}\right)\right],$$

$$\Omega^2 = \frac{k}{\rho+1}\left(k^2\sigma_T - \rho + 1\right) - \frac{k^2\rho\left(U_0^{(1)} - U_0^{(2)}\right)^2}{(\rho+1)^2},$$

$$\lambda = \frac{k\left(U_0^{(1)} - U_0^{(2)}\right)}{\rho+1}\left[\frac{4k^2}{H-1}(\rho H + \eta) + \rho q_2^{-1} - \eta q_1^{-1}\right].$$

Clearly the marginal stability can be obtained when the parameters A and λ vanish. This can be accomplished for absent $U_0^{(j)}$ or whence the two fluids move with the same velocity, in addition the damping term vanishes at the critical value H_C.

In view of the critical value (44) the damped term A will be absent from the Mathieu equation (52). Moreover, in the absence of the fluid velocity, equation (52) then reduces to

$$\frac{d^2\Theta}{dt^2} + \left[\Omega_0^2 + Q_0(J_0 + J_{00}\cos\varpi t)^2\right]\,\Theta = 0\,, \tag{53}$$

where $\Omega_0 = \lim_{U_0^{(j)}\to 0}\Omega$ and $Q_0 = \lim_{H\to H_C} Q$. Hence, we have

$$Q_0 = \frac{\mu\left[(4k^2+q_1^{-1})\eta + q_2^{-1}\right]^2 + \left[(4k^2+q_2^{-1}) + \eta q_1^{-1}\right]^2}{16k^2(\eta-1)^2(\rho^{(1)}+\rho^{(2)})}\,.$$

Equation (53) is well known as the canonical form of Mathieu's equation which is a linear differential equation with periodic coefficients. Equations similar to this equation appear in many problems in physics and applied mathematics such as stability of a transverse column subjected to a periodic longitudinal load, stability of periodic solutions of a nonlinear conservative system, electromagnetic wave propagation in a medium with periodic structure, and the excitation of certain electrical systems. The solutions of the Mathieu equation can be, under certain conditions, periodic where the system becomes stable. The condition for the periodic Mathieu functions depends on the relation between the parameters Ω_0^2 and Q_0 [39]. The $(\Omega_0^2 - Q_0)$-plane is divided into stable and unstable regions bounded by the characteristic curves of Mathieu functions. The general solution of equation (53) is stable if the point (Ω_0^2, Q_0) in the $(\Omega_0^2 - Q_0)$-plane lies in a stable region, otherwise it is unstable [39].

The stability behaviour in the static magnetic field can be discussed from equation (53) in the absence of the periodic terms, or when the parameter $J_{00} \to 0$, the stability analysis then requires that $\Omega_0^2 + Q_0 J_0^2 > 0$, which yields the following condition:

$$J_0^2 > \tilde{J} = \frac{16k^2(\eta-1)^2\,(\rho+1)\,\left(\rho - 1 - k^2\sigma_T\right)}{\mu\left[(4k^2+q_1^{-1})\eta + q_2^{-1}\right]^2 + \left[(4k^2+q_2^{-1}) + \eta q_1^{-1}\right]^2}. \tag{54}$$

This is the relation between the stratified viscosity η and the surface currents coefficient J_0. This relation occurs at the specific value for the stratified magnetic field. It is clear that surface currents will disappear from the interface whence $\eta = 1$ (i.e., $\eta^{(1)} = \eta^{(2)}$). Inspection of the above relation (54) shows that stability reveals for $\rho < 1$, in other words, whence $k^2 > \frac{\rho}{\sigma_T+1}$.

The contributions of the field frequency can be achieved in the case of nonvanishing the parameter J_{00}. Thus in the absence of the static term ($J_0 \to 0$), stability of (53) occurs when the following inequality is satisfied:

$$J_{00}^4 Q_0^2 + 16(\varpi^2 - \Omega_0^2)Q_0 J_{00}^2 + 32\Omega_0^2(\varpi^2 - \Omega_0^2) > 0\,. \tag{55}$$

It is observed that this condition is trivially satisfied when $\varpi^2 \geq \Omega_0^2$, for arbitrary Q_0 and J_{00}^2. In terms of the coefficientJ_{00}^2, the above stability condition (55) takes

the form

$$(J_{00}^2 - \tilde{J}_1)(J_{00}^2 - \tilde{J}_2) > 0\,, \tag{56}$$

where

$$\tilde{J}_{1,2} = \frac{8}{Q_0}\left[-\left(\varpi^2 - \Omega_0^2\right) \pm \sqrt{(\varpi^2 - \Omega_0^2)\left(\varpi^2 - \frac{3}{2}\Omega_0^2\right)}\right]\,. \tag{57}$$

The stable regions are characterized by the following conditions:

$$J_{00}^2 > \tilde{J}_1 \text{ and } J_{00}^2 > \tilde{J}_2\,; \quad \tilde{J}_1 > \tilde{J}_2\,. \tag{58}$$

It is clear that the two transition curves $\tilde{J}_1$ and $\tilde{J}_2$ are intersected at the point $\eta = 1$, in the plane $(J_{00}^2 - \eta)$. From Floquet theory [39], the region bounded by the two branches for the transition curves $\tilde{J}_1$ and $\tilde{J}_2$ is the unstable region; the area outside these curves is the stable region. The stability behaviour at the exact critical value of the stratified magnetic field is amplified in Figures 8 and 9. The transition curves (57) are calculated and the stability diagram shows the variation of η versus J_{00}^2. The results of increasing the field frequency ϖ and the inverse of the porous permeability q_1^{-1} on the stability criteria are shown respectively in Figures 8 and 9. In these graphs a stable zone starting from the point (1, 0) in the plane $(J_{00}^2 - \eta)$. The stable zone is surrounded by an unstable area. The width of the stable zone increases as the values of J_{00}^2 is increased. This shows the stabilizing influence of the free surface current density at the critical stratified magnetic field H_C.

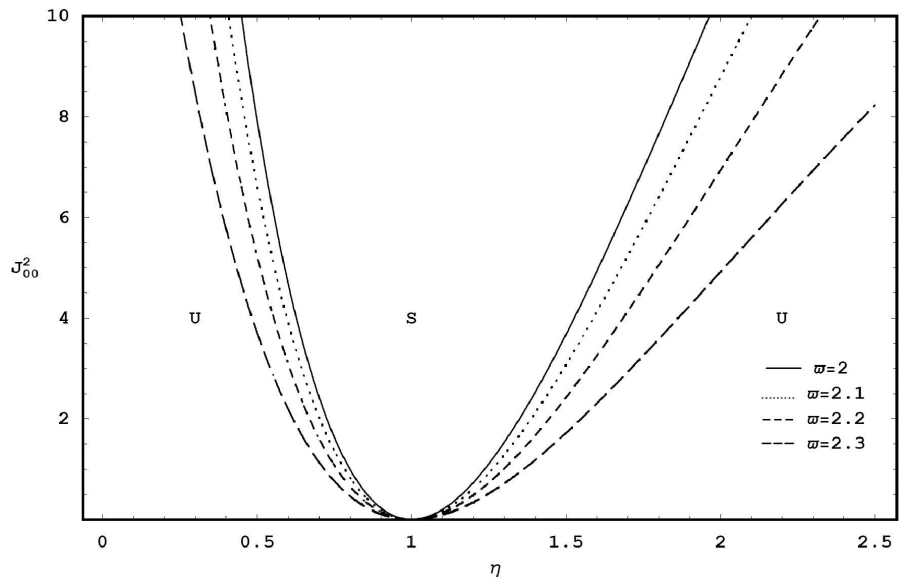

Figure 9 Influence of the field frequency ϖ on the stability configuration at the chimerical magnetic ratio H_C. The computations are made for the stability criteria (55) for a system having $\rho = 0.7, \mu = 0.5, q_1^{-1} = 1, q_2^{-1} = 1, sigma_T = 10$ at the fixed $k = 1$

In Figure 8 four consequent values of ϖ are considered. It can be noticed that the stable zone that lies at $\eta = 1$ increases in width as ϖ is increased. This shows the stabilizing influence of the field frequency. The same role was observed before in Figure 4 for the un-damped Mathieu equation (32). Another conclusion was observed in the presence of the damped term A in which the increase of ϖ has a destabilizing influence.

In Figure 9, we repeat the plot of Figure 8 by fixing the field frequency ϖ to the value $\varpi = 2$ but the permeability q_1^{-1} has some variation. It is seen that the stable zone increases in width as q_1^{-1} is increased. This shows the stabilizing influence of increasing the parameter q_1^{-1}. The same behaviour was observed before in Figure 3b).

7. Damped Effects in the Stability Behaviour

Away from the marginal stability analysis other dramatic changes in the stability behaviour can be obtained. When the growth rate solution is presented, a solution of the form $\gamma = \exp(\sigma_0 + i\omega_0)t$ occurs. Stability will depend on the sign of σ_0(the real part). If it is positive then the amplitude of the disturbance increases with time, and the flow is unstable; if it is negative then the flow is stable; and if it has a zero value then there is marginal stability.

7.1. *Stability Profile for Fluids Streaming with the Same Velocities*

In the limiting case, for fluids having the same velocities ($\lambda \to 0$), the above characteristic equation (52) reduces to the following damped Mathieu equation with real coefficients:

$$\frac{d^2\Theta}{dt^2} + A\frac{d\Theta}{dt} + \left[\Omega_0^2 + Q(J_0 + J_{00}\cos\varpi t)^2\right]\,\Theta = 0\,. \tag{59}$$

Equation (59) represents the case of the Rayleigh-Taylor problem for the Darcian fluids. This equation has, in general, a growth-rate solution. Marginal stability requires positive values of the damped term. In the other side, the periodic solution arises when the damped term vanishes.

For non-zero the damped term A and in a pure static magnetic field, equation (59) reduces to

$$\frac{d^2\Theta}{dt^2} + A\frac{d\Theta}{dt} + \left(\Omega_0^2 + QJ_0^2\right)\,\Theta = 0\,. \tag{60}$$

This is a linear differential equation with constant coefficients. For the growth rate solution, of the form $\gamma = \exp(\sigma_0 + i\omega_0)t$, both σ_0 and ω_0 is real constants and satisfies the following equations:

$$\sigma_0^2 - \omega_0^2 + A\sigma_0 + (\Omega_0^2 + QJ_0^2) = 0\,, \quad 2\sigma_0 + A = 0\,.$$

Elimination of the parameter σ_0 yields

$$\omega_0^2 = \Omega_0^2 + QJ_0^2 - \tfrac{1}{4}A^2\,. \tag{61}$$

The assumption that ω_0 is real imposes the following stability condition:

$$\Omega_0^2 + QJ_0^2 - \tfrac{1}{4}A^2 > 0\,, \tag{62}$$

with the necessary condition that A is positive. Thus the region of stability in the static case is given by

$$J_0^2 > J^{**} = \frac{1}{k^2(\mu H^2+1)}\left\{\frac{1}{4(\rho+1)}\left[4k^2(H-\eta)+ (\eta q_1^{-1}+q_2^{-1})(H-1)\right]^2 - k(H-1)^2\left[k^2\sigma_T-(\rho-1)\right]\right\}, \quad (63)$$

where $\mu = \frac{\mu^{(1)}}{\mu^{(2)}}$ is used.

The presence of the damping term A in the stability analysis that is given above leads us to estimate the contribution of the viscosity in the stability criteria. Therefore a non-dimensional parameter η^* is introduced so that $\eta^{(j)} = \eta^*\tilde{\eta}^{(j)}$, and then $A = \eta^*\tilde{A}$. The dependence of the transition curve J^{**} with respect to η^* is given by

$$\frac{\partial J^{**}}{\partial \eta^*} = \frac{\tilde{A}^2}{2Q}\eta^* . \quad (64)$$

This means that the unstable region bounded by the curve J^{**} increases in size as η^* is increased, which shows that an increase in the viscosity parameter has a destabilizing influence.

For a non-zero the periodic coefficient J_{00} and the static part J_0 is ignored, equation (59) is reduced to

$$\frac{d^2\Theta}{dt^2} + A\frac{d\Theta}{dt} + \left(\Omega_0^2 + QJ_{00}^2\cos^2\varpi t\right)\Theta = 0 . \quad (65)$$

There are many books that have dealt with equation (65) (see e.g. Grimshaw [40]). The small and positive coefficient A is described as a function of the coefficient of the period term. Grimshaw [40] examined, using a perturbation technique, the first unstable region, which occurs near $\Omega_0^2 = \varpi^2 + \frac{1}{4}A^2 - \frac{1}{2}QJ_{00}^2$. On the boundaries of this unstable region, there is periodic solution of (65) of period 2π. The stability condition is thus given by

$$3Q^2J_{00}^4 - 16(\varpi^2-\Omega_0^2)QJ_{00}^2 + 16(\varpi^2-\Omega_0^2)^2 + 16\varpi^2A^2 > 0 . \quad (66)$$

Clearly, the disappearance of free electric surface currents from the fluid interface occurs whence $A \to 0$ and the field frequency ϖ^2 has the same value of Ω_0^2. It is clear that there is a critical value for which the damped term A is absent; this critical value is given by (44). The relation H_C occurs at the marginal stability case. In other words, the relation (44) can be reformulated as

$$k_C^2 = \frac{(H-1)(\eta q_1^{-1}+q_2^{-1})}{4(\eta-H)} . \quad (67)$$

This means that disappearance of J_{00}^2 will occur at a specific value of the wavenumber as defined above by (67). This point is known as the resonance point which occurs when $\varpi^2 = \Omega_0^2$.

The presence of a positive damped term has not altered the position of the stability boundary for the un-damped Mathieu equation in the stability diagram in

the (J_{00}^2, k)-plane. For each fixed $A > 0$, in the (J_{00}^2, k)-plane, there is a hyperbola bounding the unstable region and does not contact the $k-$axis. These boundaries are described by

$$J_{1,2}^{**} = \frac{4}{3Q}\left[2(\varpi^2 - \Omega_0^2) \pm \sqrt{(\varpi^2 - \Omega_0^2)^2 - 3\varpi^2 A^2}\right]. \tag{68}$$

Hence the stability criteria (68) cab be satisfied whence

$$J_{00}^2 > J_1^{**} \text{ and } J_{00}^2 < J_2^{**}; \quad J_1^{**} > J_2^{**}.$$

The two transition curves J_1^{**} and J_2^{**} will be calculated for some numerical values. These two transition curves should bound an unstable region and be surrounded by a stable area.

In the present calculations we show the plots in the plane (J_{00}^2, k) for the case of the Rayleigh-Taylor problem in the presence of the viscous damped coefficient A. The results of the calculations for the transition curves (68) are shown in Figures 11–13a), and b). In Figure 11 we examine the effect of the field frequency ϖ on the stability criteria. Some consequent values of ϖ are considered and displayed in the graph. It is noticed that the unstable region has shifted up associated with an increase in its width as ϖ is increased. This shows the destabilizing influence of increasing the field frequency ϖ. Another observation was found in the previous graph of Figure 4 in the case of moving the fluids.

The influence of the stratified viscosity η on the stability behaviour is the subject of the graph of Figure 10. In this investigation two different roles are observed for increasing the parameter η. It is seen that as η is increased from the value $\eta = 1$ to the value $\eta = 1.1$, the width of the unstable region increases and moves down. This means that the increase in η has a destabilizing influence. Maximum instability occurs as η reaches the value $\eta = 1.2$. A continuous increase in η to the value 1.3 leads to a decrease the width of the unstable region and a shift up. When η has the value 1.4, more decrease in the width has achieved and more moving up. Hence the values of $\eta > 1.2$ play a stabilizing influence in the stability behaviour.

The examination of increasing the upper permeability parameter q_1 has been displayed in Figure 13a) and b) for some consequent values. In Figure 13a) the examination is done for a specific value of the stratified viscosity having the value $\eta = 1.1$. In Figure 13b) we repeated the same calculation of Figure 13a) but for another fixed value for the stratified viscosity $\eta = 1.4$. It appears that the increase in q_1^{-1} leads to an increase in the width of the unstable region where $\eta = 1.1$ and a decrease in the width occurs whence $\eta = 1.4$. This means that the parameter q_1^{-1} plays a stabilizing role in Figure 13a) and a destabilizing role in Figure 13b). The same conclusion is observed when we increase the lower permeability parameter q_2. Hence there are two different roles for the resistance force that has been achieved in the present calculations.

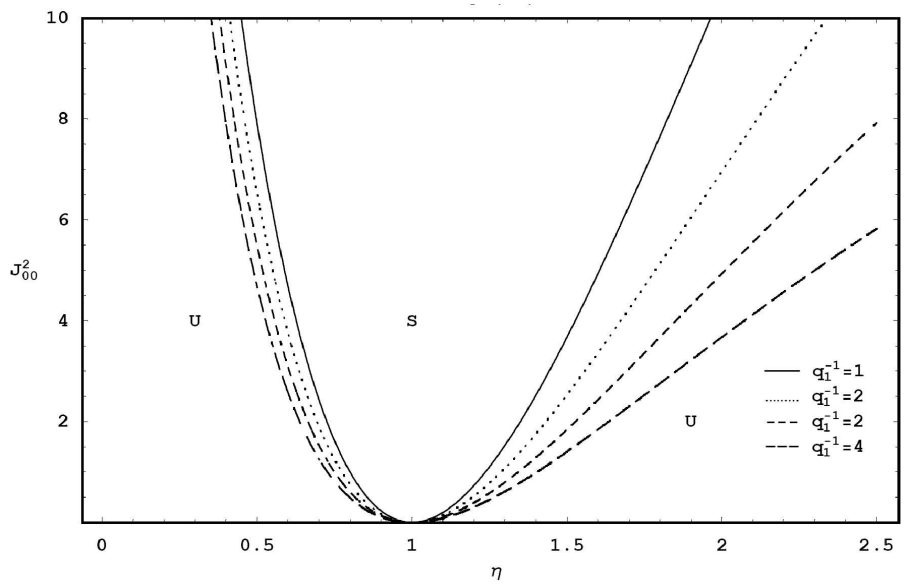

Figure 10 For the same system as in Fig. 9 for variation the porous permeability q_1^{-1}

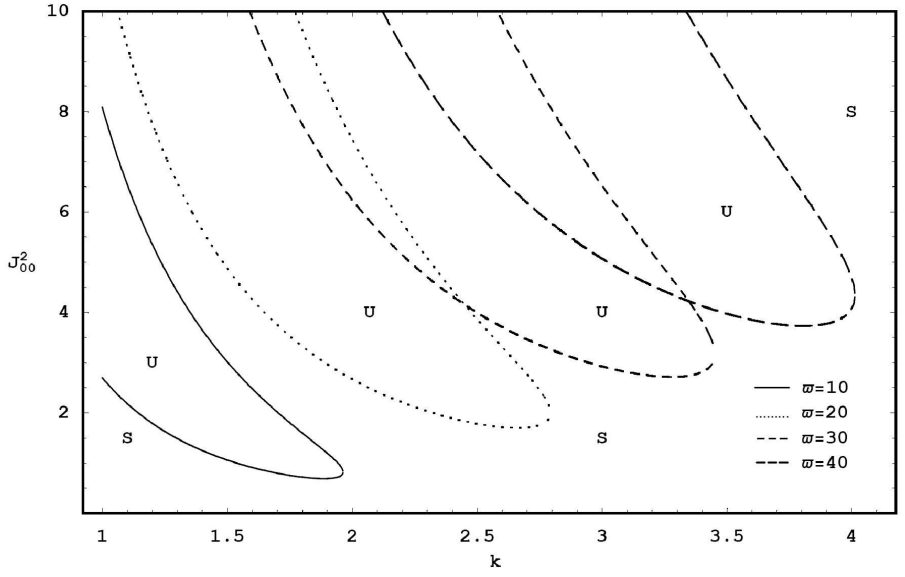

Figure 11 Represents the stability criteria (66) for a system having $\rho = 0.7$, $\eta = 1.3$, $\mu = 1.5$, $\varpi = 10, 20, 30, 40$, $q_1^{-1} = 1$, $q_2^{-1} = 1$ and a fixed value for the magnetic field ratio $H = 1.2$

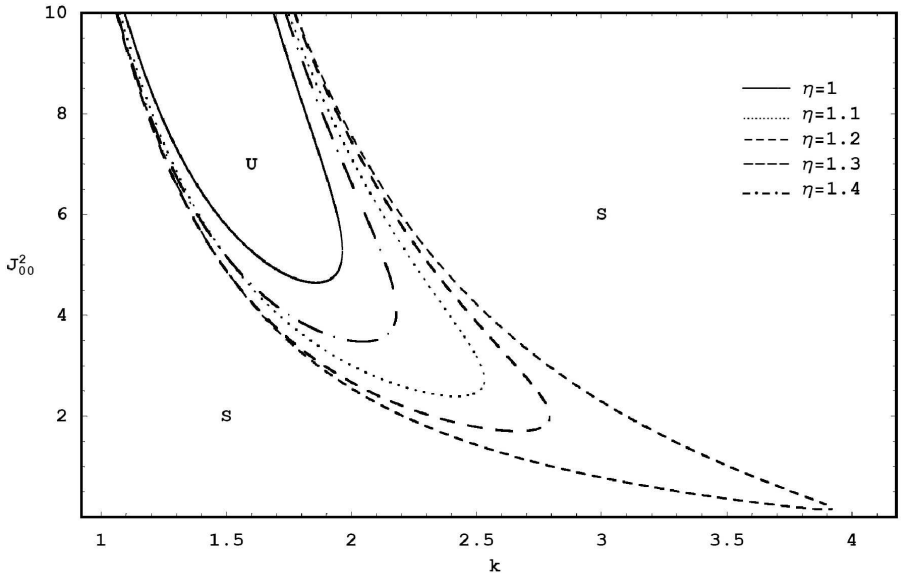

Figure 12 For the same system as in Fig. 11 except that the field frequency has a fixed value $\varpi = 10$ and the viscosity ratio has some variation

7.2. *Kelvin-Helmholtz Instability in the Presence of Damped Effects*

The parameterλ of Mathieu equation (52) can vanish even when the velocity field $U_0^{(1)}$ and $U_0^{(2)}$ are non-zero and having non-equal values. This can be accomplished for a special value of the stratified magnetic field. This value is given by

$$H_S = \frac{\rho q_2^{-1} - \eta q_1^{-1} - 4k^2\eta}{(4k^2 + q_2^{-1})\rho - \eta q_1^{-1}}. \tag{69}$$

At this special value equation (52) has a following simplified form:

$$\frac{d^2\Theta}{dt^2} + A_* \frac{d\Theta}{dt} + \left[\Omega^2 + Q_* \left(J_0 + J_{00}\cos\varpi\, t\right)^2\right]\, \Theta = 0, \tag{70}$$

where $A_* = \lim_{H\to H_S} A$ and $Q_* = \lim_{H\to H_S} Q$, hence, we have

$$\begin{aligned} A_* &= \frac{\eta}{\eta+\rho}\left(4k^2 + q_1^{-1} + q_2^{-1}\right)\,, \\ Q_* &= -\frac{\mu\left[\rho q_2^{-1} - \eta q_1^{-1} - 4k^2\eta\right]^2 + \left[(4k^2 + q_2^{-1})\rho - \eta q_1^{-1}\right]^2}{4(\rho+1)(\rho+\eta)\left[(4k^2 + q_2^{-1})\rho - \eta q_1^{-1}\right]}\,. \end{aligned}$$

For non-zero the damped term and in a pure static magnetic field, the region of stability is given by

$$J_0^2 > J_c = \frac{1}{Q_*}(\frac{1}{4}A_*^2 - \Omega^2)\,, \tag{71}$$

which is the stability behaviour for the damping equation (70) as $J_{00} \to 0$.

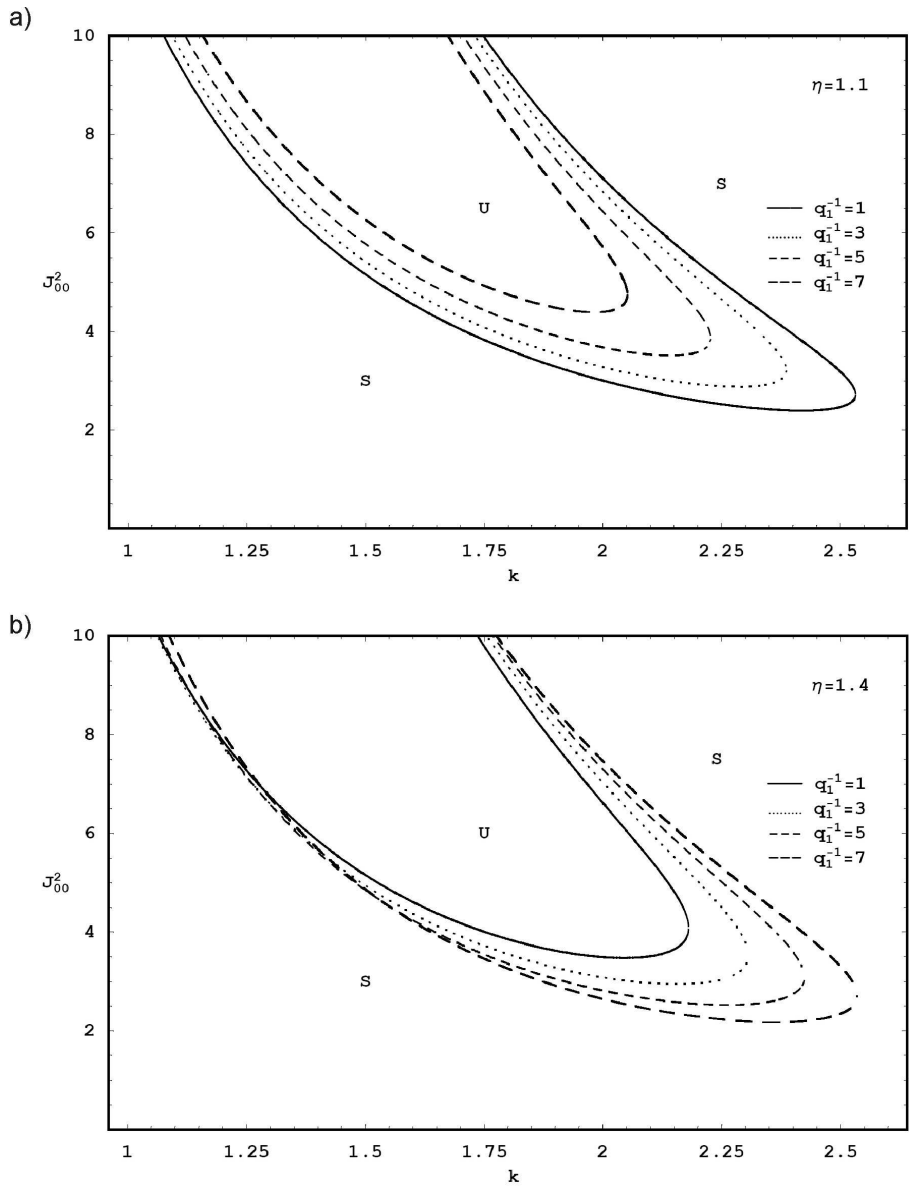

Figure 13 Represents some consequence values for the parameter q_1^{-1} at a fixed value of $\eta = 1.1$ for the same system as in Fig.12; b): represents some consequence values for the parameter q_1^{-1} at a fixed value of $\eta = 1.4$ for the same system as in Fig. 12

For a non-zero the periodic coefficient J_{00} and the static part J_0 is ignored, the stability condition is thus given by

$$3Q_*^2 J_{00}^4 - 16(\varpi^2 - \Omega^2)Q_* J_{00}^2 + 16(\varpi^2 - \Omega^2)^2 + 16\varpi^2 A_*^2 > 0\,. \tag{72}$$

Namely

$$(J_{00}^2 - J_a)(J_{00}^2 - J_b) > 0, \tag{73}$$

$$J_{a,b} = \frac{4}{3Q_*}\left[2(\varpi^2 - \Omega^2) \pm \sqrt{(\varpi^2 - \Omega^2)^2 - 3\varpi^2 A_*^2}\right]. \tag{74}$$

The region lies between the two branches of J_a and J_b represents the destabilizing region sandwiched in the stabilizing area.

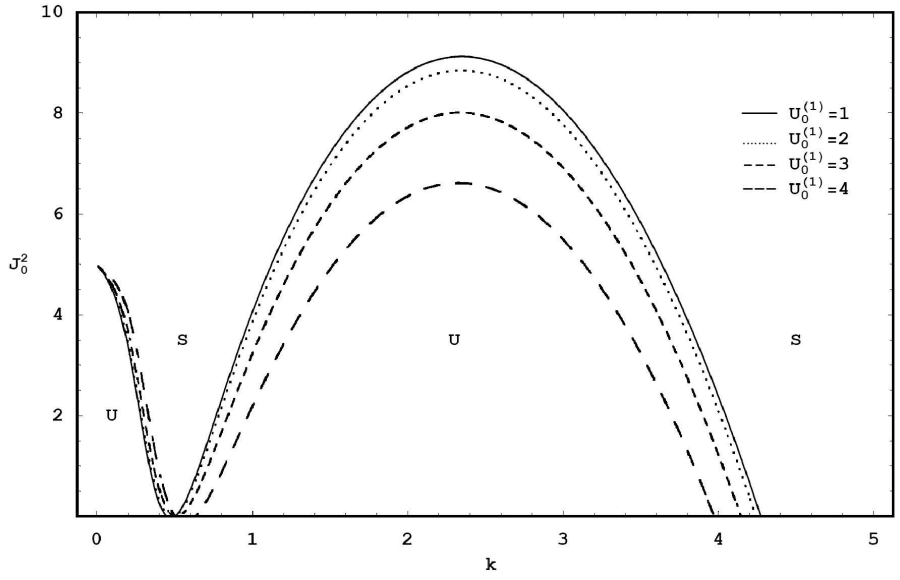

Figure 14 Represents the stability criteria 71) for a system having $\rho = 0.5$, $\eta = 1$, $\mu = 0.6$, $q_1^{-1} = 1$, $q_2^{-1} = 1$, $U_0^{(2)} = 1$, $\sigma_T = 12$

The dependence of the special value of the stratified magnetic field H_S on the stability behaviour in the static case is shown in Figures 14, 15 and 16. The numerical result has been done for the stability criteria (71). The transition curve in these graphs participate the plane into stable and unstable regions. Inspection of the stability diagram shows that the free electric surface currents will disappear from the interface between the fluids for $k = k_1$ and $k = k_2$, where

$$k_1 = \sqrt{\frac{\eta q_1^{-1} - \rho q_2^{-1}}{4\rho}}, \tag{75}$$

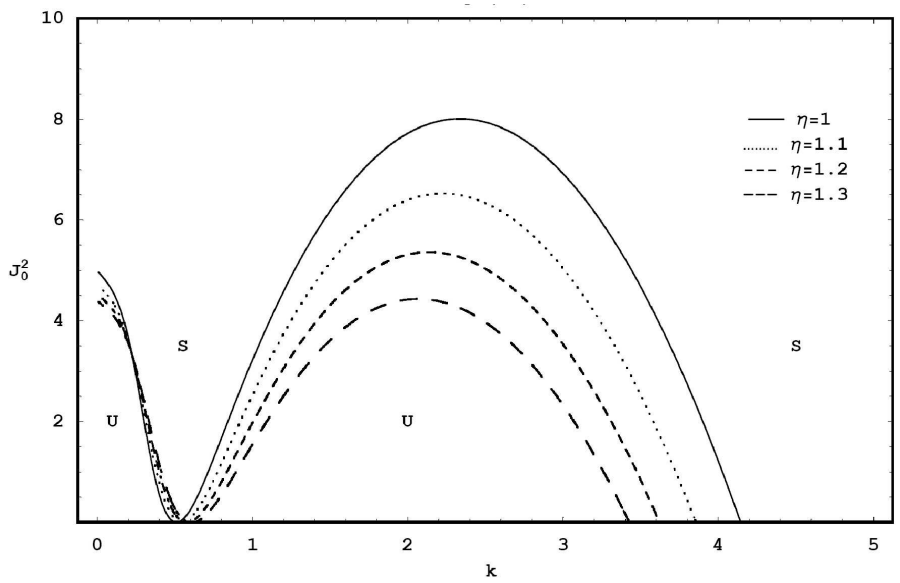

Figure 15 The same as in Fig. 14 except that $U_0^{(1)} = 3$ and some variation for the viscosity ratio is considered

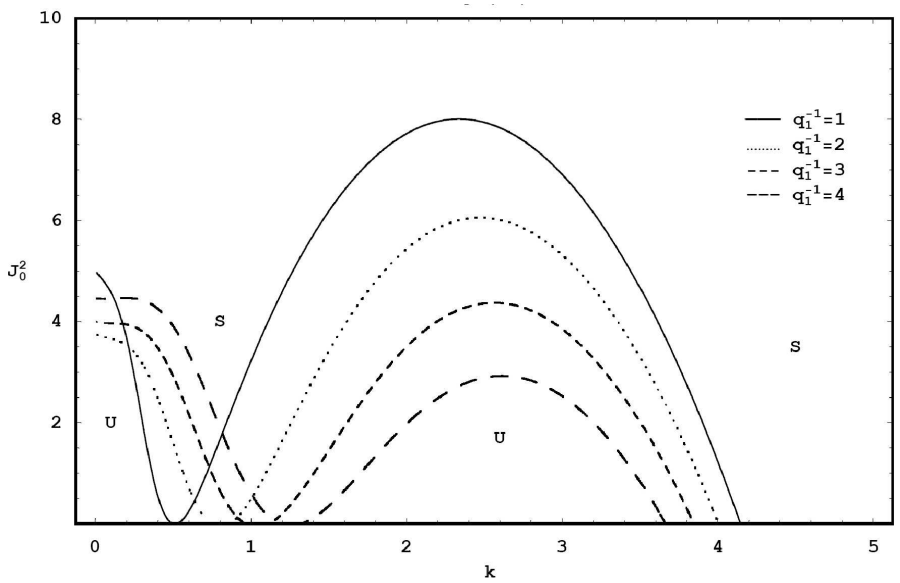

Figure 16 Refers to the same system as in Fig.15 except that some consequence values of the porous permeability is considered

$$k_2^4 - \frac{\sigma_T(\eta+\rho)^2}{4\eta^2(\rho+1)}k_2^3 + \left[\frac{1}{2}\left(q_1^{-1}+q_2^{-1}\right) + \frac{\rho(\eta+\rho)^2\left(U_0^{(1)}-U_0^{(2)}\right)^2}{4\eta^2(\rho+1)^2}\right]k_2^2 + \frac{(\rho-1)(\eta+\rho)^2}{4\eta^2(\rho+1)}k_2 + \left(q_1^{-1}+q_2^{-1}\right)^2 = 0\,. \quad (76)$$

The examination of the variation of the velocity $U_0^{(1)}$, the viscosity ratio η and the permeability parameter q_1^{-1} on the stability criteria is displayed in Figures 14, 15 and 16 respectively. It appears that the increase in $U_0^{(1)}$, η and q_1^{-1} decreases the unstable region. It is seen that these parameters play of a stabilizing role at the critical stratified magnetic field in the absence of the field frequency. Other different behaviours are found for investigation in the presence oscillating the magnetic field. The numerical computation for the stability criteria (72) is made and has been illustrated in Figures 17, 18 and 19. The dependence on the variation of the velocity $U_0^{(1)}$ on the stability behaviour is the subject of Figure 17. It appears that, in the presence of the field frequencyϖ, the increase in $U_0^{(1)}$ increases the unstable zone. This shows that velocity plays a destabilizing role. In Figure 18 we repeated the computation for variation of the viscosity parameter. It is found that the increase of the viscosity ratio η leads to a decreases in the width of the unstable zone. Similar behaviour is observed when we increase the permeability q_1^{-1}. Therefore both η and q_1^{-1} have a damping effect in the stability criteria in the presence of the field frequency.

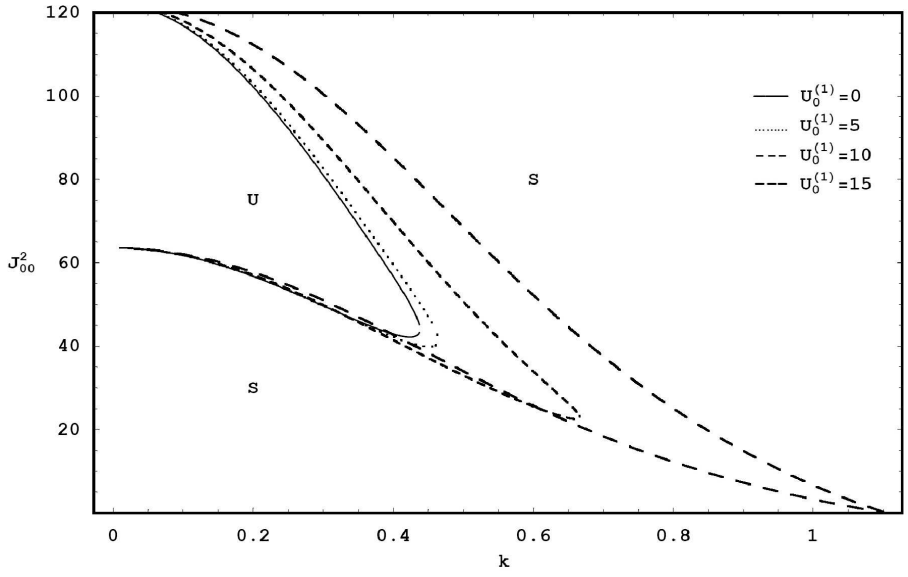

Figure 17 Refers to the transition curves (74) for a system having $\rho = 0.5$, $\eta = 1.5$, $\mu = 2.5$, $\varpi = 5$, $q_1^{-1} = 2$, $q_2^{-1} = 1$, $U_0^{(2)} = 1$, $\sigma_T = 10$

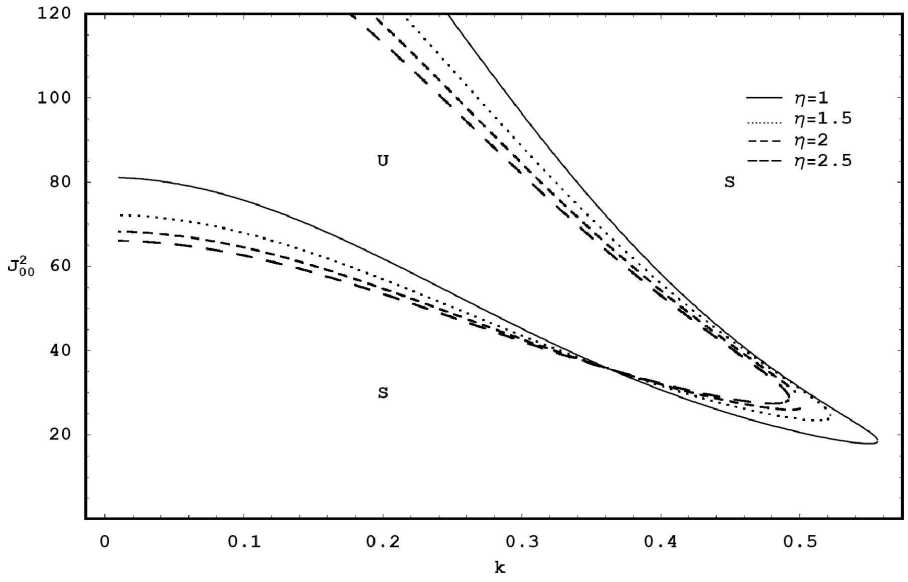

Figure 18 For the same system as in Fig. 17 except that $U_0^{(1)} = 3$

8. Stability Behaviour for the Full Complex Damped Mathieu Equation (52)

In this section, we return to the full complex damped Mathieu equation (52). We shall deal with the general case where the growth rate disturbance is presented. In the case of a uniform magnetic field, Hurwitz stability criterion is used. The necessary and sufficient conditions for stability is given by

$$A > 0 \text{ and } A^2(\Omega^2 + QJ_0^2) - \lambda^2 > 0\,. \tag{77}$$

Thus the negative of the real part of the growth rate holds as the above conditions are satisfied. The transition curve separating the stable from the unstable regions is given by

$$J_0^2 > J^{\otimes} = \frac{1}{QA^2}(\lambda^2 - A^2\Omega^2)\,. \tag{78}$$

To determine the stability conditions for the complex damped Mathieu equation (50), a perturbation technique may be used to accomplish this purpose. We use the method of multiple scales as described by [27, 32] to obtain an approximate solution and to analyze the stability criteria.

Since we are considering the surface deformations caused by the magnetic surface stress stemming from the alternating external magnetic field, it would be convenient to recall an ordering relation $J_{00}^2 = \varepsilon J_0^2$, with J_0 as a constant of proportionality.

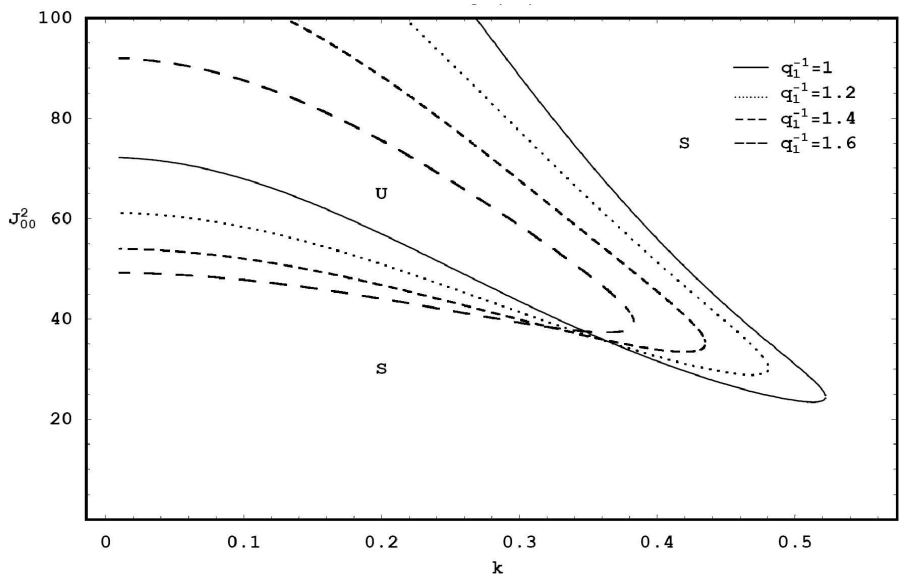

Figure 19 For the same system as in Fig. 18 for variation q_1^{-1}

In accordance with the method of multiple time scales, two time scales T_0 and T_1 are introduced:

$$T_0 = t \text{ and } T_1 = \varepsilon t\,.$$

The differential operators can now be expressed as the derivative expansions

$$\frac{d}{dt} = \frac{\partial}{\partial T_0} + \varepsilon \frac{\partial}{\partial T_1} + \dots, \text{ and } \frac{d^2}{d\,t^2} = \frac{\partial^2}{\partial T_0^2} + 2\varepsilon \frac{\partial^2}{\partial T_0 \partial T_1} + \dots,$$

where T_0 is time of the lowest order. The detailed analysis of this procedure is given in [32]. Omitting the details, one finds the stability criterion at the resonance case of approaching the field frequency ϖ to the frequency part $\hat{\omega}$ of the growth disturbance in the form

$$J_{00}^2 < J_1^{\otimes} = \frac{4(\varpi - \hat{\omega})(4\hat{\omega}^2 + A - 2\Omega^2)}{Q(2\hat{\omega} + \sqrt{3\Omega^2 - 2\hat{\omega}^2 - \frac{3}{4}A^2})}\,, \tag{79}$$

$$J_{00}^2 > J_2^{\otimes} = \frac{4(\varpi - \hat{\omega})(4\hat{\omega}^2 + A - 2\Omega^2)}{Q(2\hat{\omega} - \sqrt{3\Omega^2 - 2\hat{\omega}^2 - \frac{3}{4}A^2})}\,, \tag{80}$$

where $\hat{\omega}$ is the disturbance frequency given by

$$\hat{\omega}^2 = \tfrac{1}{8}\left(4\Omega^2 - A^2 + \sqrt{(4\Omega^2 - A^2)^2 + 16\lambda^2}\right)\,. \tag{81}$$

From the Floquet theory [39], the region bounded by the two branches of the transition curves $J_1^{\otimes}$ and $J_2^{\otimes}$ is the unstable region. The region outside these curves is

stable. The width of the unstable region is represented by $(J_2^{\otimes} - J_1^{\otimes})$. The increase of this refers to the destabilizing influence, while its decrease represents a stabilizing role. The contact between $J_1^{\otimes}$ and $J_2^{\otimes}$ refers to the resonance point. This point occurs when field frequency ϖ approaches disturbance frequency $\hat{\omega}$. Investigating the two transition curves $J_1^{\otimes}$ and $J_2^{\otimes}$ reveals that the resonance point occurs for $J_{00}^2 = 0$. However this resonance point can be given by

$$\lambda^2 + (4\Omega^2 - A^2)\varpi^2 - 4\varpi^4 = 0. \tag{82}$$

In terms of the ratio H, the above equation can be put in the following form:

$$aH^2 + 2bH + c = 0, \tag{83}$$

where

$$\begin{aligned}
a &= k^2\left(U_0^{(1)} - U_0^{(2)}\right)^2\left(4k^2\rho + \rho q_2^{-1} - \eta q_1^{-1}\right)^2 + 4k\varpi^2(\rho+1)\left(k^2\sigma_T - \rho + 1\right) - \\
&\quad 4k^2\rho\varpi^2\left(U_0^{(1)} - U_0^{(2)}\right)^2 - \varpi^2\left(4k^2 + q_2^{-1} + \eta q_1^{-1}\right)^2 - 4\varpi^4(\rho+1)^2, \\
b &= k^2\left(U_0^{(1)} - U_0^{(2)}\right)^2\left(4k^2\rho + \rho q_2^{-1} - \eta q_1^{-1}\right)\left(4k^2\eta - \rho q_2^{-1} + \eta q_1^{-1}\right) - \\
&\quad 4k\varpi^2(\rho+1)\left(k^2\sigma_T - \rho + 1\right) + 4k^2\rho\varpi^2\left(U_0^{(1)} - U_0^{(2)}\right)^2 + \\
&\quad \varpi^2(4k^2 + q_2^{-1} + \eta q_1^{-1})(4k^2\eta + q_2^{-1} + \eta q_1^{-1}) + \varpi^4(\rho+1)^2, \\
c &= k^2\left(U_0^{(1)} - U_0^{(2)}\right)^2\left(4k^2\eta - \rho q_2^{-1} + \eta q_1^{-1}\right)^2 + 4k\varpi^2(\rho+1)(k^2\sigma_T - \rho + 1) - \\
&\quad 4k^2\rho\varpi^2\left(U_0^{(1)} - U_0^{(2)}\right)^2 - \varpi^2\left(4k^2\eta + q_2^{-1} + \eta q_1^{-1}\right)^2 - 4\varpi^4(\rho+1)^2.
\end{aligned}$$

Therefore, for each real positive values of the roots H_1^* and H_2^* of the above equation (83), there are two resonance points at $(H_1^*, 0)$ and $(H_2^*, 0)$.

We present the numerical discussion for the stability behaviour where the magnetic field depends of the frequency ϖ. Therefore the computation is made for the transition curves (79) and (80). In the calculations the computed value of the free electric surface currents parameter J_{00}^2 versus the ratio H at a fixed the wavenumber k is utilized. In these calculations the stability picture at the resonance case of $\varpi \approx \hat{\omega}$ is presented. The numerical results are displayed in Figures 20–23. In these calculations two resonance points are found and they satisfy the condition $\varpi = \hat{\omega}$. The transition curves that are imbedded from these resonance points have bounded the unstable resonance regions. The two unstable regions are connected and collected into one unstable region. Outside the resonance region is the stable region. It is observed that the resonance region is a function of both ϖ, ρ, η, $U_0^{(j)}$, q_j^{-1} and k.

In Figure 20 we examine the influence of the field frequency on both the resonance points and the unstable resonance region. The graph is computed for some consequent values for the frequency ϖ, while other parameters are held fixed. For a

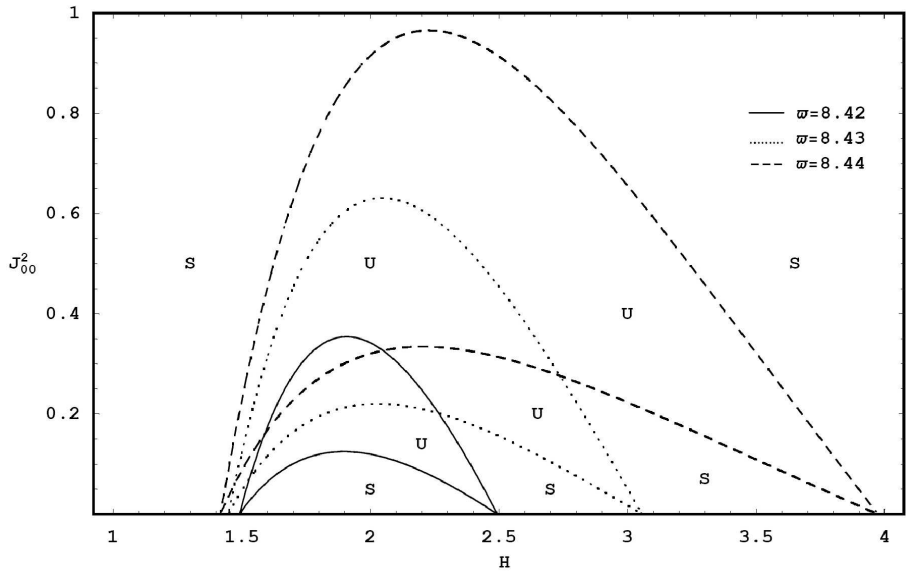

Figure 20 Represents the transition curves of (78) and (79) for a system having $\rho = 1.2$, $\eta = 0.7$, $\mu = 0.6$, $q_1^{-1} = 5$, $q_2^{-1} = 1$, $U_0^{(1)} = 3$, $U_0^{(2)} = 1$, $\sigma_T = 80$ for a fixed the wavenumber at $k = 1.3$

specific frequency $\varpi = 8.42$, it is found the first resonance point lies at $H = 1.49094$ while the second resonance located at $H = 2.49472$. When the frequency has been increased to the value $\varpi = 8.43$, the first resonance shifts to the position $H = 1.44814$ and the second resonance point shifts to $H = 3.05709$. In the case of $\varpi = 8.44$, the first resonance lies at the point of $H = 1.41789$, while the second resonance is located at $H = 3.974$. Thus we conclude that as ϖ is increased the distance $(H_1^* - H_2^*)$ increases. Moreover, the width of the unstable region increases. This shows the destabilizing influence of increasing the field frequency ϖ.

In Figure 21 we repeated the calculations of Figure 20 but for some variation of the viscosity parameter η. The other physical parameters are held fixed. It is seen that as η is changed from the value 0.7 to the value 0.75 the width of the unstable region has decreased. Another conclusion is observed whence η is increased to the value 0.8, the width of unstable region increases. This means that there is a dual role in the stability behaviour at the resonance case as the viscosity ratio is increased.

The influence of some variation of the fluid velocity $U_0^{(1)}$ and the permeability parameter q_1^{-1} are the subject of Figure 22 and Figure 23, respectively. It appears that the increase in both $U_0^{(1)}$ and q_1^{-1} have a destabilizing influence in the stability behaviour at the resonance case.

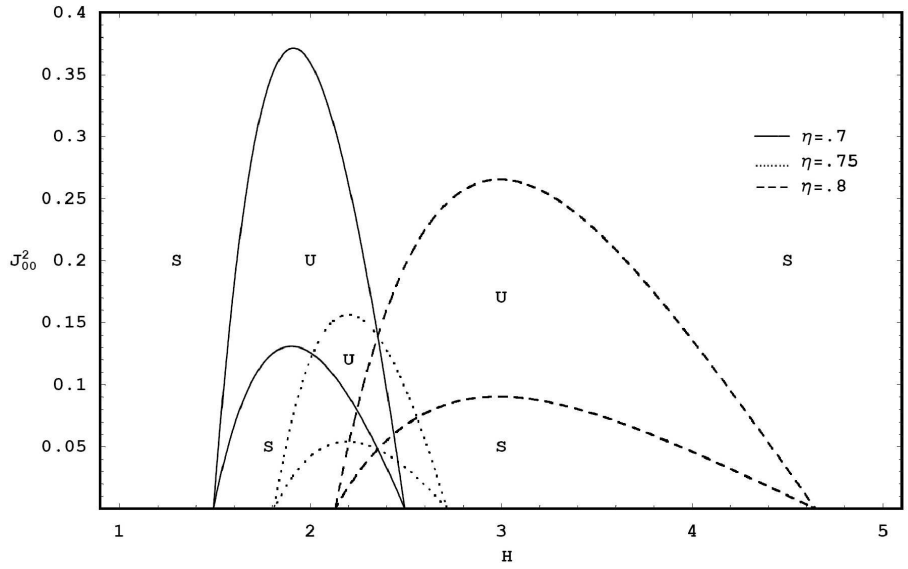

Figure 21 For the same system as in Fig. 20 except that $\varpi = 8.42$ and $\eta = 0.7\,, 0.75\,, 0.8$

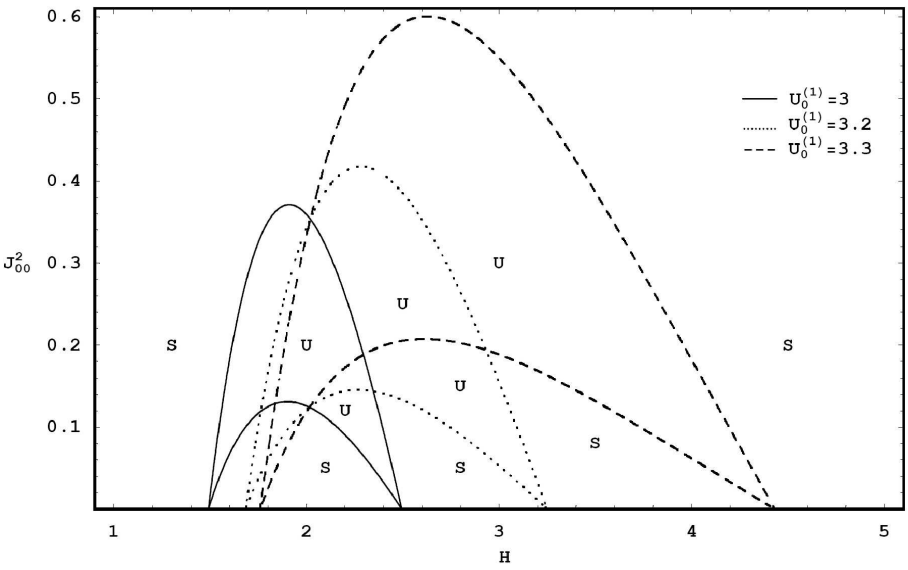

Figure 22 For the same system as in Fig. 20 with $\varpi = 8.42$ and $\eta = 0.7$

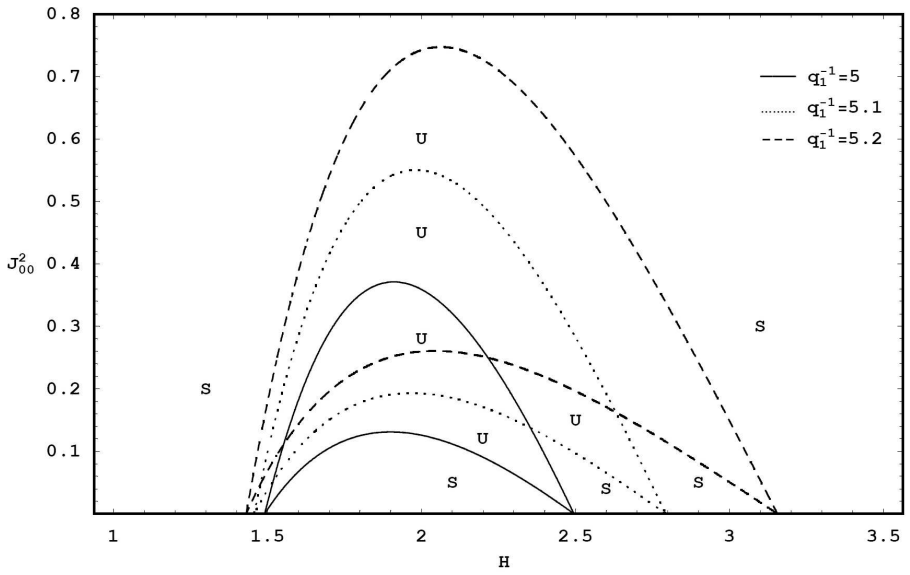

Figure 23 For the same system as in Fig. 20 but q_1^{-1} has some consequence values

References

[1] **Chandrasekhar, S**: *Hydrodynamic and Hydromagnetic Stability*, (1961), Oxford Univ. Press, Oxford.

[2] **Fertman, VE**: *Magnetic Fluids Guidebook*, (1990), Hemisphere, Washington.

[3] **Zakaria, K**: *Physica A*, (1999), **273**, 248.

[4] **Rosensweig, R E**: *Ferrohydrodynamics*, (1985), Cambridge, Cambridge University Press.

[5] **Zelazo, RE** and **Melcher, JR**: *J. Fluid Mech.*, (1969), **39**, 1.

[6] **Drazin, PG**: *J. Fluid Mech.*, (1970), **42**, 321.

[7] **Nayfeh, AH**, and **Saric, WS**: *J. Fluid Mech.*, (1972), **55**, 311.

[8] **Weissman, MA**: *Phil. Trans. R. Soc. A*, (1979), **290**, 639.

[9] **Melcher, JR**: *Field Coupled Surface Waves*, MIT Press, Cambridge, MA. *Continuum electromechanics*, (1981), MIT Press, Cambridge, MA.

[10] **El-Dib, YO**, *J. Plasma Phys.*, (1996), **55**, 219.

[11] **El-Dib, Y** and **Matoog, RT**: J. Colloid Interface Sci, **229**, (2000), 29.

[12] **El-Dib, YO**: *J. Physica Scripta*, (2002), **66**, 308.

[13] **Dullien, FAL**: *Fluid Transport and Pore Structure*, (1992), Academic Press, New York.

[14] **Bear, J** and **Bachmat, Y**: *Introduction to modelling of transport phenomena in porous media*, (1991), Kluwer Academic, Dordrecht.

[15] **Baranblatt, GI**, **E'tov, VM** and **Ryzhik, VM**: *Theory of fluid through natural rocks*, (1990), Kluwer Academic, Dordrecht.

[16] **Sharma, RC** and **Spanos, TJT**: *Can. J. Phys.*, (1982), **60**, 1391.

[17] **Raghaven, R** and **Mardsen, SS**: *Q. J. Mech. Appl. Math.*, (1973) **26**, 205.

[18] **Bau, HH**: *Phys. Fluids*, (1982), **25**, 1719.

[19] **Gheorghitza StI**: *Bull. Math. Soc. Sci. Math. R. S. Roum.*, (1967), **11**, 25; *J. Sci. Eng. Res.*, (1969), **13**, 39.

[20] **Georgescu, A** and **Gheorghitza, StI**: *Rev. Roum. Math. Pure Appl.*,(1971), **16**, 27.

[21] **El-Sayed, MF**: *Can. J. Phys.*, (1997), **75**, 499.

[22] **Mohamed, AA**, **El-Dib, YO** and **Mady, AA**: *Chaos, Solitons and Fractals*, (2002), **14**, 1027.

[23] **El-Dib, YO** and **Ghaly, AY**: *J. of Colloid and Interface Science*, (2004), **269**, 224.

[24] **El-Dib, YO** and **Ghaly, AY**: *Chaos Solitons & Fractals*, (2003), **18**, 55.

[25] **El-Dib, YO**: *J. Magnetism and Magnetic Materials*, (2003), **260**, 1.

[26] **El-Dib, YO**: *J. of Colloid and Interface Science*, (2003), **259**, 409.

[27] **Nayfeh, AH** and **Mook, DT**: *Nonlinear Oscillations*, (1979), Jonh Wiley & Sons, Inc. Virginia.

[28] **El-Dib, YO**: *J. Plasma Physics*, (2001), **65**, 1.

[29] **El-Dib, YO** and **Moatimud, GM**: *Z. Naturforsch*, (2002), **57a**, 159.

[30] **Mohamed, AA**, **Elshehawey, EF** and **El-Dib, YO**: *J. Colloid Interface Sci,*, (1998), **207**, 54.

[31] **El-Dib, YO**: *ZAMP*, (1997), **48**, 60.

[32] **El-Dib, YO**: *J.Phys. A Math. Gen.*, (1997), **30**, 3585.

[33] **El-Dib, YO**: *Chaos, Solitons and Fractals*, (2001), **12**, 705.

[34] **Nield, DA** and **Bejan, A**: *Convection in Porous Media*, (1992), New York, Springer-Verlag.

[35] **Woodson, HH**, and **Melcher, JR**: *Electromechanical Dynamics*, (1968), John Wiley & Sons.

[36] **Batchelor, GK**: An introduction to Fluid Dynamics" (Cambridge University Press, Cambridge, UK., (1967).

[37] **Landau, LD** and **Lifshitz, EM**: *Electrohydrodynamics of Continuous Media*, (1960), Pergamon Press. Oxford.

[38] **Morse, PM** and **Feshbach, H**: *Methods of Theoretical Physics I*, (1953), McGraw-Hill, New York.

[39] **Mclachlan, NW**: *Theory and Application of Mathieu Functions*, (1964), Dover, New York.

[40] **Grimshaw, R**: *Nonlinear Ordinary Differential Equations*, (1990), Blackwell, Oxford.